

# Proglacial lake development and outburst flood hazard at Fjallsjökull glacier, southeast Iceland

Greta H. Wells<sup>1,2</sup>, Þorsteinn Sæmundsson<sup>1,3</sup>, Finnur Pálsson<sup>1</sup>, Guðfinna Aðalgeirsdóttir<sup>1</sup>, Eyjólfur Magnússon<sup>1</sup>, Reginald L. Hermanns<sup>4,5</sup>, Snævarr Guðmundsson<sup>6</sup>

<sup>1</sup> Institute of Earth Sciences, University of Iceland, Reykjavík, 101, Iceland  
<sup>2</sup> School of Geosciences, University of Edinburgh, Edinburgh, EH8 9XP, UK  
<sup>3</sup> Faculty of Life and Environmental Sciences, University of Iceland, Reykjavík, 101, Iceland  
<sup>4</sup> Geological Survey of Norway, Trondheim, 7040, Norway  
<sup>5</sup> Norwegian University of Science and Technology, Trondheim, 7491, Norway  
<sup>6</sup> South East Iceland Nature Research Center, Höfn, 780, Iceland

*Correspondence to:* Greta H. Wells (ghwells@hi.is)

# Proglacial lake development and outburst flood hazard at Fjallsjökull glacier, southeast Iceland

30 Wells, Greta H.<sup>1,2</sup>, Sæmundsson, Þorsteinn<sup>1,3</sup>, Pálsson, Finnur<sup>1</sup>, Aðalgeirsdóttir, Guðfinna<sup>1</sup>, Magnússon, Eyjólfur<sup>1</sup>, Hermanns, Reginald L.<sup>4,5</sup>, Guðmundsson, Snævarr<sup>6</sup>

<sup>1</sup> Institute of Earth Sciences, University of Iceland, Reykjavík, 101, Iceland

<sup>2</sup> School of Geosciences, University of Edinburgh, Edinburgh, EH8 9XP, UK

35 <sup>3</sup> Faculty of Life and Environmental Sciences, University of Iceland, Reykjavík, 101, Iceland

<sup>4</sup> Geological Survey of Norway, Trondheim, 7040, Norway

<sup>5</sup> Norwegian University of Science and Technology, Trondheim, 7491, Norway

<sup>6</sup> South East Iceland Nature Research Center, Höfn, 780, Iceland

*Correspondence to:* Greta H. Wells (ghwells@hi.is)

40 **Abstract.** Glacier retreat is projected to continue with ongoing climate change, elevating the risk of mass movement-triggered glacial lake outburst floods (GLOFs). These events are an emerging yet understudied hazard in Iceland, including at Fjallsjökull, an outlet glacier of the Vatnajökull ice cap in southeast Iceland. The proglacial Fjallsárlón lake significantly expanded from 1945 to 2021, enabling measurements of lake depth and volume changes with a multibeam sonar scanner. This lake bathymetry, coupled with radio-echo sounding surveys of subglacial topography, makes it possible to estimate future lake  
45 development. If recent glacier terminus retreat rates continue, Fjallsárlón is estimated to reach its maximum extent within the next one to two centuries, more than doubling in surface area and tripling in volume. The lake will occupy two overdeepened basins with a maximum depth of ~210 m, which will likely increase terminus melting and calving rates—and thus glacier retreat—as well as potentially float the glacier tongue. Three zones on the valley walls above Fjallsjökull have high topographic potential of sourcing rock falls or avalanches that could enter Fjallsárlón and generate displacement waves that could exit the  
50 lake as GLOFs, impacting visitors and infrastructure at this popular tourism site. This study offers an assessment of mass movement-triggered GLOF hazard at Fjallsárlón—the first time this emerging risk has been investigated in Iceland. Results provide high-resolution multibeam sonar measurements of lake bathymetry that can inform additional studies on glacier–lake interactions, GLOF risk mitigation strategies, and selection of priority sites for monitoring and additional mapping at Fjallsárlón. This study also offers a methodology for assessing this hazard at other proglacial sites in Iceland and worldwide  
55 with rapidly expanding lakes and growing potential societal impacts.

## 1. Introduction and aims

Glaciers worldwide have retreated rapidly over the past century, and this rate is projected to continue with ongoing climate change (Hock et al., 2019; Zemp et al., 2019; Marzeion et al., 2020; Hugonnet et al., 2021; Rounce et al., 2023). Proglacial lakes often form in front of retreating glacier termini, particularly where ice has eroded overdeepened troughs into  
60 bedrock and sediment, and these lakes are growing in size and number as glaciers retreat worldwide (Cook and Swift, 2012;

Carrivick and Tweed, 2013; Haeberli et al., 2016; Shugar et al., 2020; Zhang et al., 2024). Proglacial lakes can drain suddenly and catastrophically in jökulhlaups (also referred to as glacial lake outburst floods or GLOFs) if their dams are breached by displacement waves generated by a mass movement event—such as a rapid rock slope failure, ice avalanche, or landslide—that enters the lake (Evans and Clague, 1994; Westoby et al., 2014a; Haeberli et al., 2017; Harrison et al., 2018). These mass movements may be triggered by paraglacial processes, such as glacier debuitressing, freeze–thaw activity, or stress adjustments from post-glacial crustal unloading and rebound, as well as permafrost degradation and thaw, seismic activity, extreme precipitation or snowmelt events, and ice crevassing and avalanching (Gruber and Haeberli, 2007; McColl, 2012; Stoffel and Huggel, 2012; Krautblatter et al., 2013; Korup and Dunning, 2015; Krautblatter and Leith, 2015; Deline et al., 2021, 2022; Ballantyne, 2022). Moreover, these processes can act in positive feedback loops. Glacial lake deepening increases terminus melt and calving rates (Carrivick et al., 2020; Sutherland et al., 2020), and glacial lake expansion increases the lake surface area where mass movements can enter and the water volume that can be displaced (Emmer et al., 2020).

GLOFs can significantly impact landscapes and societies far downstream of the source lake, leaving a geomorphologic legacy that persists over long time scales (Carrivick and Tweed, 2016; Larsen and Lamb, 2016; Wells et al., 2022; Emmer, 2023; Lützow et al., 2023; Morey et al., 2024). GLOFs may also trigger hazard cascades by entraining material to transform into debris flows, undercutting channel banks to increase likelihood of subsequent collapse, and depositing material to dam new lakes at risk of draining (Korup and Tweed, 2007; Worni et al., 2014; Allen et al., 2022b; Geertsema et al., 2022). Mass movements into proglacial lakes have triggered GLOFs across the globe, including in the Himalaya–Hindu Kush (Richardson and Reynolds, 2000), Andes (Hubbard et al., 2005), Patagonia (Harrison et al., 2006), Canadian Cordillera (Clague and Evans, 2000), and Iceland (Kjartansson, 1967), as well as tsunamis in marine fjords in Greenland (Svennevig et al., 2020), Norway (Hermanns et al., 2006), and Alaska (Higman et al., 2018).

Projected atmospheric temperature rise is expected to increase glacier retreat, proglacial lake expansion, and paraglacial activity in Iceland, heightening the threat of mass movement-triggered GLOFs, though this emerging hazard remains understudied. Though jökulhlaups occur more frequently in Iceland than nearly anywhere else on Earth, most have been triggered by subglacial volcanic and geothermal activity (Björnsson, 2002; Dunning et al., 2013; Carrivick and Tweed, 2019; Magnússon et al., 2021) or ice dam flotation or failure (Thorarinsson, 1939; Roberts et al., 2005). Rapid glacier retreat and thinning is occurring in Iceland, with a  $16 \pm 4\%$  decrease in ice volume since 1890 (Aðalgeirsdóttir et al., 2020; Belart et al., 2020; Hannesdóttir et al., 2020) and a projected additional loss of at least 20% by 2100 for its largest ice caps (Flowers et al., 2005; Aðalgeirsdóttir et al., 2011; Schmidt et al., 2020; Compagno et al., 2021; Rounce et al., 2023). Proglacial lakes have expanded since they began to form in the early 20<sup>th</sup> century and now occur in front of most southern outlet glaciers at Vatnajökull, Iceland’s largest ice cap (Guðmundsson et al., 2019). Mass movements partly attributed to paraglacial processes have fallen onto several outlet glaciers in Iceland in the past century, including Steinsholt sjökull (1967), an outlet glacier of the Eyjafjallajökull ice cap (Kjartansson, 1967), Jökulsárgílsjökull (1972) (Sigurðsson and Williams, 1991) and Tungnakvíslarjökull (2003), outlet glaciers of the Mýrdalsjökull ice cap, and Morsárjökull (2007) (Sæmundsson et al., 2011) and Svínafellsjökull (2013) (Ben-Yehoshua et al., 2022), outlet glaciers of the Vatnajökull ice cap (Fig. 1A and 1B); and

95 ongoing surface deformation is observed above Tungnakvíslarjökull (Lacroix et al., 2022) and Svínafellsjökull (Ben-Yehoshua et al., 2023). Despite many locations of activity, only one known mass movement has triggered a GLOF in Iceland—the rockslide onto the Steinsholtjökull outlet glacier in 1967, which fractured glacial ice and slid into the proglacial lake, where it generated a displacement wave that continued downstream as a flood and debris flow (Kjartansson, 1967).

One site with favorable conditions for mass-movement triggered GLOFs is Fjallsjökull, an outlet glacier of the  
100 Vatnajökull ice cap in southeast Iceland that is located in Vatnajökull National Park (Fig. 1C). Fjallsjökull is rapidly retreating in a steep-walled valley with an overdeepened trough and is in contact with the proglacial Fjallsárlón lake. A mass movement-triggered GLOF from Fjallsárlón could have a significant societal impact since the lake is one of Iceland’s most visited glacier tourism sites—attracting more than 260,000 visitors in 2022 (Þórhallsdóttir, 2023)—and is situated ~1 km west of Route 1, which is the only land route connecting eastern and western Iceland on the south coast. This study conducts an assessment of  
105 mass movement-triggered GLOF scenarios at Fjallsárlón—the first time this emerging hazard has been investigated in Iceland. Specifically, it addresses the questions: how will Fjallsárlón develop under ongoing climate change, and how will this evolution influence GLOF risk from mass movement events into the lake? This paper: 1) presents results of a 2020 lake bathymetric survey with a multibeam sonar scanner; 2) reconstructs lake volume changes from 1945 to 2021; 3) estimates future lake and glacier development; and 4) identifies potential sources of mass movements and discusses resulting displacement wave or  
110 GLOF scenarios at Fjallsárlón. Results provide input data for additional studies on glacier–lake interactions, inform risk assessments, and prioritize sites for mapping and monitoring to mitigate GLOF hazard at Fjallsárlón. This study also offers a methodology for assessing this emerging hazard at other proglacial lakes worldwide where growth in potential GLOF risk is outpacing the speed of research.

## 2. Study area and background

115 Fjallsjökull is an outlet glacier of the southern part of Örafajökull, a central volcano that lies beneath the Vatnajökull ice cap in southeast Iceland (Fig. 1B). Fjallsjökull reached its maximum historical extent in the 18<sup>th</sup> and 19<sup>th</sup> centuries (Thorarinsson, 1943; Bradwell, 2004). The glacier was connected with the Breiðamerkurjökull outlet glacier to the north and Hrútárjökull outlet glacier to the south, but the ice had retreated enough to separate into different termini by 1945 and 2010, respectively (Fig. 1C) (Hannesdóttir et al., 2015; Guðmundsson et al., 2019). Between ~1890 and 2010, the glacier lost ~23%  
120 of its surface area and ~35% of its volume (Hannesdóttir et al., 2015). Bedrock maps from radio-echo sounding surveys show that Fjallsjökull occupies two overdeepened troughs carved into bedrock and sediment reaching maximum depths of ~205 m and ~120 m below sea level (Magnússon et al., 2012). The glacier is bounded by the Breiðamerkurfjall mountain to the north and the Ærfjall mountain to the south (Fig. 1C). Approximately 5 km from the present-day terminus, the glacier flows over a series of bedrock steps that create ice falls (Magnússon et al., 2012). Small proglacial lakes began to form in front of Fjallsjökull  
125 in 1936, one of which eventually became Fjallsárlón (Howarth and Price, 1969; Guðmundsson et al., 2019). Since its first appearance in aerial photographs and maps in 1945, the lake surface area expanded from ~0.5 km<sup>2</sup> to ~3.7 km<sup>2</sup> in 2018

(Guðmundsson et al., 2019). Point surveys conducted with a weighted rope (and echo-sounder in 1966) revealed a maximum lake depth of 45 m in 1951, 58 m in 1966, 66 m in 2006, and 119 m in 2016 (Howarth and Price, 1969; Magnússon et al., 2007; Guðmundsson et al., 2019). A neighboring glacial lake, Breiðarlón, drains into Fjallsárlón via the Breiðá river.

130 Fjallsárlón's outlet is the Fjallsá river, which flows for ~8 km southeast across a sandur to the Atlantic Ocean (Fig. 1C).

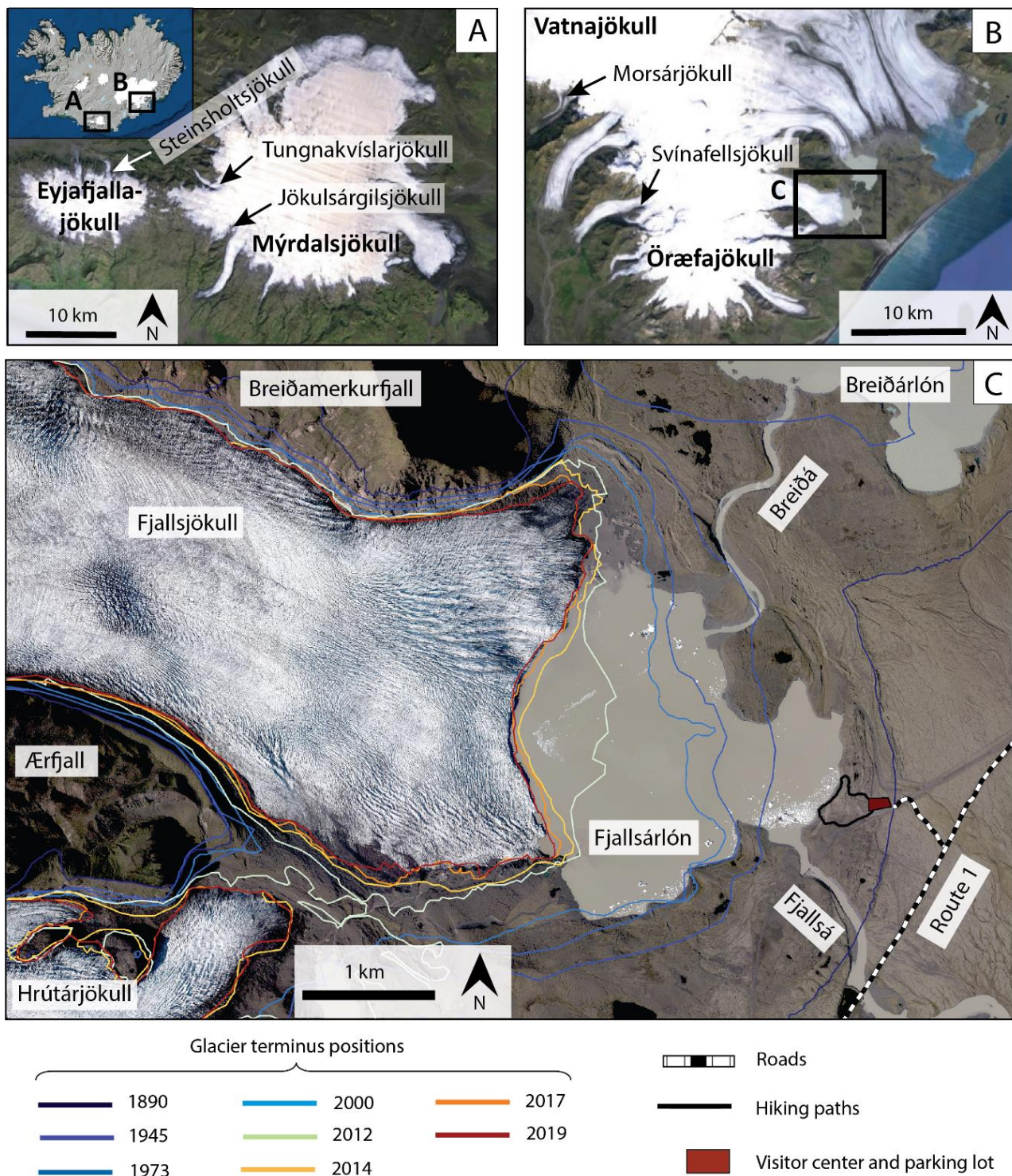


**Figure 1. Map of study area and selected locations of historic mass movements onto glaciers in Iceland that are mentioned in the main text. (A) Mýrdalsjökull and Eyjafjallajökull ice caps (Google Earth basemap); (B) Örfajökull**

135 **volcano beneath Vatnajökull ice cap (Google Earth basemap); (C) Fjallsjökull glacier and Fjallsárlón lake in 2021 with glacier terminus positions at eight time steps between 1890 and 2019 (glacier outlines obtained from Hannesdóttir and Guðmundsson (2024)). Basemap photo from 2021 (Loftmyndir ehf., 2022).**

The glacier foreland contains landform assemblages characteristic of active temperate glacial landsystems, including moraines, till, hummocky terrain, and glacial and glaciofluvial sediments and deposits (Evans and Twigg, 2002; Chandler et al., 2020). Bedrock in the area is predominantly subaerially erupted basalt (formed during interglacial periods) and subglacially  
140 erupted basalt including hyaloclastite, breccia, and pillow lava (formed during glacial periods) that date to ~0.7 to 2.7 million years and older (Stevenson et al., 2006; Roberts and Gudmundsson, 2015). Some plutonic rocks also occur in Breiðamerkurfjall at the northern margin of Fjallsjökull (Hauksdóttir et al., 2021). Despite Iceland's subarctic location, regional climate is mild and maritime due to influence from the warm Irminger Current. Mean annual temperature near the glacier terminus is ~5° C (measured at the Fagurhólsmýri weather station ~20 km southwest of Fjallsárlón from 1949 to 2023), and mean annual  
145 precipitation is ~3500 mm (measured at the Kvísker station approximately 6 km southwest of Fjallsárlón from 1962 to 2011) (Icelandic Meteorological Office, 2024).

### 3. Methods

#### 3.1. Bathymetric survey and bed DEM

A bathymetric survey was conducted in August 2020 using a Teledyne RESON SeaBat T20-P multibeam sonar  
150 scanner (420 kHz) attached to a small, motorized boat. GNSS data was collected with a Trimble SPS-852 land survey rover on-board and RTK base station close to the lakeshore, yielding a relative accuracy of  $\pm 3$  cm in vertical and horizontal directions. Multibeam sonar scanner results were corrected for sound wave velocity changes based on water temperature and depth, though sound velocity profile measurements were limited to a depth of 35 m, and the presence of icebergs and subglacial streams were sources of interference, adding uncertainty to vertical measurements. However, given that sound velocity changes  
155 by  $1.7 \text{ m s}^{-1}$  for every 100 m depth and  $4 \text{ m s}^{-1}$  for every  $1^\circ \text{ C}$  (Friðriksson, 2014), we can estimate changes of at least  $1.7 \text{ m s}^{-1}$  based on measured maximum lake depth and at least  $4 \text{ m s}^{-1}$  based on observed temperature variations in nearby proglacial lakes with similar settings. Lake surface elevation was measured at a point along the shoreline at the time of the bathymetric survey with a Trimble TCS-3 (Trimble 852 reference station) and a survey stick and reported as 5 m above sea level (m a.s.l.) following correction for above-geoid height (ISN93 coordinate system).

160 To create a continuous topographic digital elevation model (DEM) of the Fjallsjökull area (hereafter referred to as the bed DEM), three datasets were combined: 1) bathymetric data from the multibeam sonar survey; 2) subglacial topography measured with radio-echo sounding surveys by the Institute of Earth Sciences, University of Iceland in 2005–2006, interpolated from point measurements (vertical uncertainty of point measurements  $\pm 20$  m) (Magnússon et al., 2012); and 3) ÍslandsDEM, a DEM of subaerial topography created from an airborne lidar survey in 2010–2011 (vertical uncertainty  $<0.5$  m) (Jóhannesson  
165 et al., 2013; Landmælingar Íslands, 2021). These datasets were mosaicked together using Surfer®, version 13 (Golden



Software, LLC, 2015), with which all subsequent data processing and calculations were carried out. Since the bathymetric survey could not cover the entire lake extent due to shallow water, floating icebergs, and proximity to the calving terminus, data gaps between the surveyed area and 2021 lakeshore outline were interpolated via kriging.

### 3.2. Glacier terminus evolution

170 Fjallsjökull terminus positions for eight time steps between 1890 and 2019 were retrieved from the Icelandic Glacier  
Web Portal (Hannesdóttir and Guðmundsson, 2024) and originally derived from remote sensing imagery, lidar DEMs, maps,  
and field measurements (Hannesdóttir et al., 2015, 2020; Guðmundsson et al., 2019). The 2021 terminus was manually  
digitized from an aerial photograph from Loftmyndir ehf. (Loftmyndir ehf., 2022) (Fig. 1C). Glacier terminus retreat rates  
were calculated using the rectilinear box method, which captures Fjallsjökull's asymmetric terminus shape (Lea et al., 2014;  
175 Dell et al., 2019). Following the methodology presented in Moon and Joughin (2008) and Howat and Eddy (2011), we drew a  
rectangular box that included maximum terminus locations between 1890 and 2021 and had an arbitrary boundary roughly  
500 m up-glacier from the minimum (2021) terminus position. For each year, we calculated glacier-covered area within the  
box; measured the areal differences between successive time steps; and divided area change by box width (approximately  
perpendicular to glacier flow line) to estimate average horizontal terminus retreat distance during the time interval. Finally,  
180 we divided retreat distances by the number of years in the time interval to estimate the average annual horizontal retreat rate  
across the terminus. Future glacier terminus retreat rate was estimated using the annual average retreat rate from 2000–2021,  
which captures glacier response to an atmospheric temperature increase in Iceland after ~1995, a trend that we expect to  
continue with future atmospheric warming (Björnsson et al., 2013; Aðalgeirsdóttir et al., 2020). To estimate a range of glacier  
scenarios, we selected two additional terminus retreat rates: 1) a rate that is approximately double the 2000–2021 rate, which  
185 represents the relative influences of increased atmospheric warming (Bosson et al., 2023) and increased lake depth if the  
terminus retreats into the deeper overdeepened trough; and 2) a rate that is approximately half the 2000–2021 rate, which  
reflects the relative influence of the Blue Blob, a region of cooling in the North Atlantic Ocean that has slowed Icelandic  
glacier retreat rates since 2011 and is projected to continue until ~2050 (Noël et al., 2022). Taken together, these three rates  
were used to estimate terminus positions at decadal intervals from 2030–2120, assuming that rates continue linearly and all  
190 parts of the terminus retreat at the same rate.

### 3.3. Lake surface area and volume calculations

Lake surface area and volume were calculated for 20 time steps between 1945 and 2021 using the bed DEM and  
digitized lake outlines. Outlines for 1945–2018 were obtained from Guðmundsson et al. (2019) and were originally derived  
from aerial photographs, satellite images, lidar DEMs, maps, and field observations. The 2021 outline was digitized from an  
aerial photograph from Loftmyndir ehf. (Loftmyndir ehf., 2022) (Fig. 2). Though there are no reported lake surface elevation  
195 measurements prior to 2020, digitized lake outlines show that the eastern, northern, and southern shorelines have remained in  
similar positions since the first aerial photograph of Fjallsárlón was taken in 1945, indicating a relatively stable surface



elevation; thus, we used the 2020 measured lake surface elevation to estimate future evolution. Future lake extents were estimated for ten time steps between 2030 and 2120 by digitizing the outline of the 2021 lake shoreline, then extending it up-valley along the 5 m a.s.l. contour line to each projected glacier terminus position, assuming that terminus retreat will continue linearly at the 2000–2021 rate and the 2020 lake surface elevation will remain constant. Lake surface area and volume were then calculated for each estimated future lake outline using the bed DEM. Past and future lake volumes assume that sedimentation is negligible in Fjallsárlón.

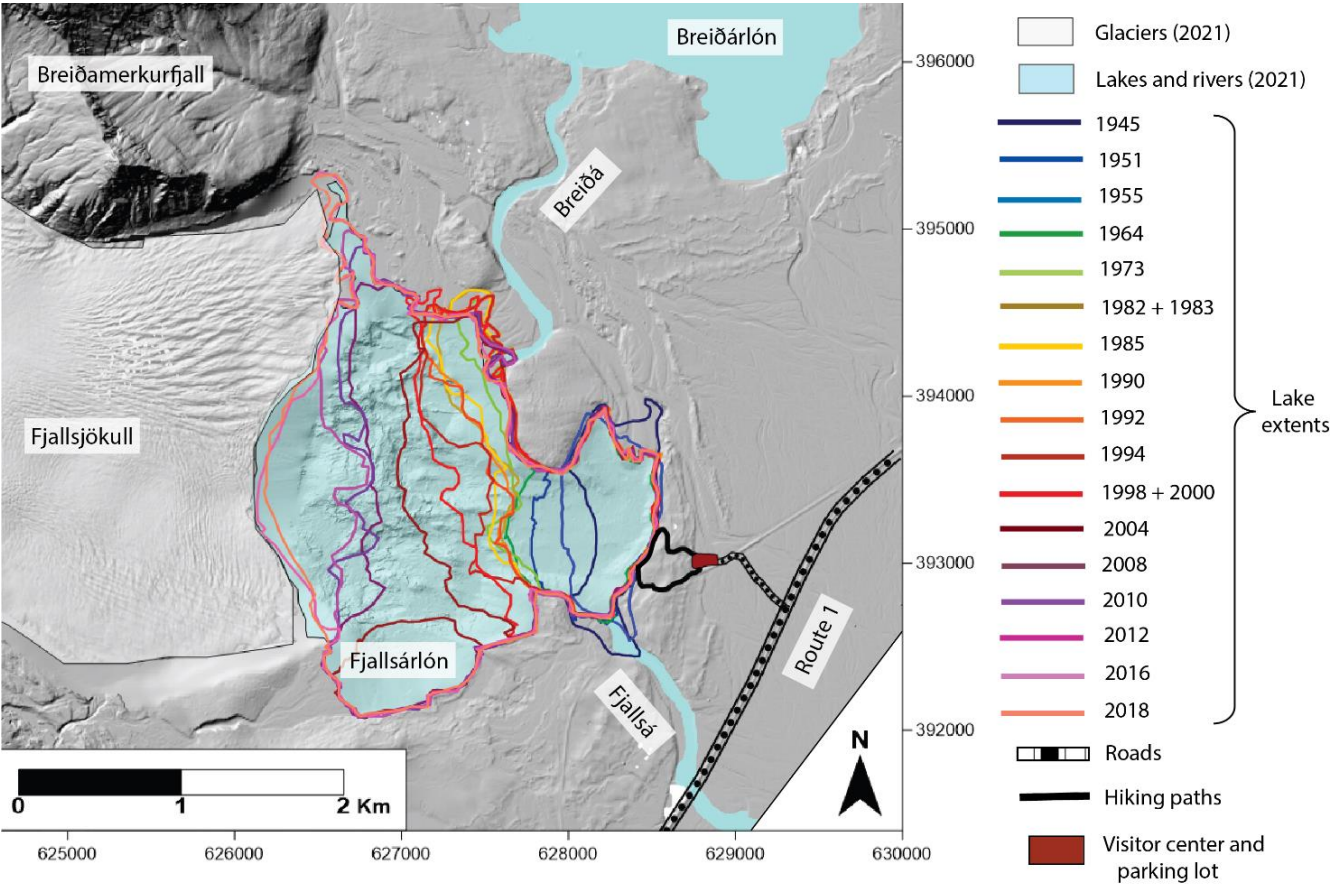


**Figure 2.** Fjallsárlón lake extents for 20 time steps between 1945 and 2021 (lake outlines obtained from Guðmundsson et al. (2019) and a 2021 aerial photo from Loftmyndir ehf. (2022)). Bed DEM basemap with ISN93 coordinate system.

### 3.4. Mass movement potential and glacial lake outburst flood threat

Slope angle and vertical elevation of the valley walls above Fjallsjökull were mapped using the ÍslandsDEM basemap (Landmælingar Íslands, 2021) in ArcGIS Pro (version 3.2.0) and the bed DEM. To identify areas with a higher potential of sourcing a mass movement, we delineated zones that met two criteria: 1) slope angles  $>30^\circ$ , which numerous

studies have defined as a critical threshold for slopes more prone to failure (Romstad et al., 2009; Allen et al., 2019; Emmer et al., 2020; Penna et al., 2022); and 2) vertical relief >200 m, which are expected to yield enough material to significantly impact the glacier or lake below (Böhme et al., 2022; Matthew et al., 2024). In each of the identified zones, we evaluated the potential of a mass movement reaching the glacial lake—and thus potentially triggering a GLOF—by measuring four parameters based on glacier and lake positions in 2021 and when the lake has reached its estimated maximum future extent: 1) maximum vertical height (vertical distances from the highest point in the zone to the 2021 glacier surface at the zone base or to the assumed future lake surface of 5 m a.s.l.); 2) horizontal travel distance (horizontal distances from the midpoint of the zone’s lowest boundary to the 2021 glacier terminus or estimated future lakeshore along the shortest straight-line path); 3) H/L ratio and angle of reach (fahrböschung; defined as  $\tan^{-1}(H/L)$ ), which are slightly modified from the classical definitions by using the distance to the glacier terminus or lakeshore rather than the distance to the lowest deposit point along the estimated flow path, thus representing scenarios where the mass movement enters the lake (not necessarily where the material is deposited) (H = maximum height difference between the highest zone point and the lake surface elevation of 5 m a.s.l.; L = horizontal length between the highest zone point and the terminus or lakeshore); and 4) horizontal distance between the highest and lowest zone boundaries (Fig. 3) (Hermanns et al., 2022). Taken together, these measurements provide a first order assessment of the topographic potential for valley walls to produce mass movements that could trigger a GLOF from Fjallsárlón (Hermanns et al., 2013; Allen et al., 2019; Emmer et al., 2020; Zheng et al., 2021). We also calculated glacier surface gradient along the central flow line from below the ice fall to the 2021 terminus using a 2021 glacier DEM (Belart and Magnússon, 2024). Finally, we looked for evidence of previous mass movement events in aerial photos from 2003, 2015, 2019, and 2021 (Loftmyndir ehf., 2022) and 1982 and 1998 (Landmælingar Íslands, 2022).

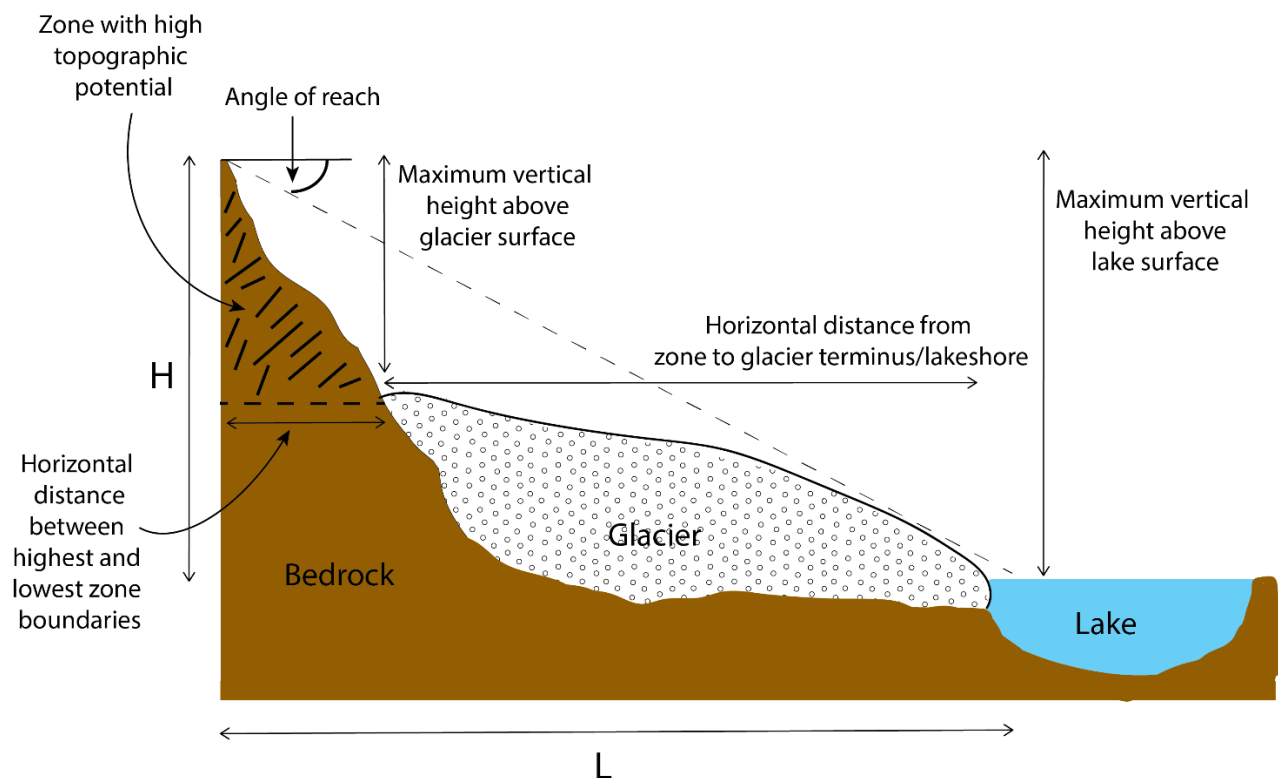


**Figure 3. Schematic diagram of topographic parameters measured to assess the potential of a mass movement event entering a glacial lake.**

## 4. Results

### 4.1. Topography of the Fjallsjökull area

The subglacial topography reveals two overdeepened troughs beneath Fjallsjökull (Fig. 4). In 2021, the southern trough was occupied partly by Fjallsárlón and partly by Fjallsjökull and reached a maximum depth of 123 m below sea level. The second trough, which is located at the northern valley margin near Breiðamerkurfjall, reaches a maximum depth of 205 m below sea level and is currently under Fjallsjökull, with the deepest point ~1.3 km from the 2021 terminus (Magnússon et al., 2012). A higher-elevation ridge reaching a maximum depth of ~20 m below sea level separates the two overdeepenings. Maximum lake depth increased from 32 m in 1945 to 128 m since 2016, when Fjallsjökull retreated into the deepest section of the southern trough (Table 1). Lake depths derived from the bathymetric sonar survey generally correspond well with point depth measurements taken in 2016, as well as radio-echo sounding results from 2005–2006 in the area that was covered by ice at the time of the survey but is now in the lake.

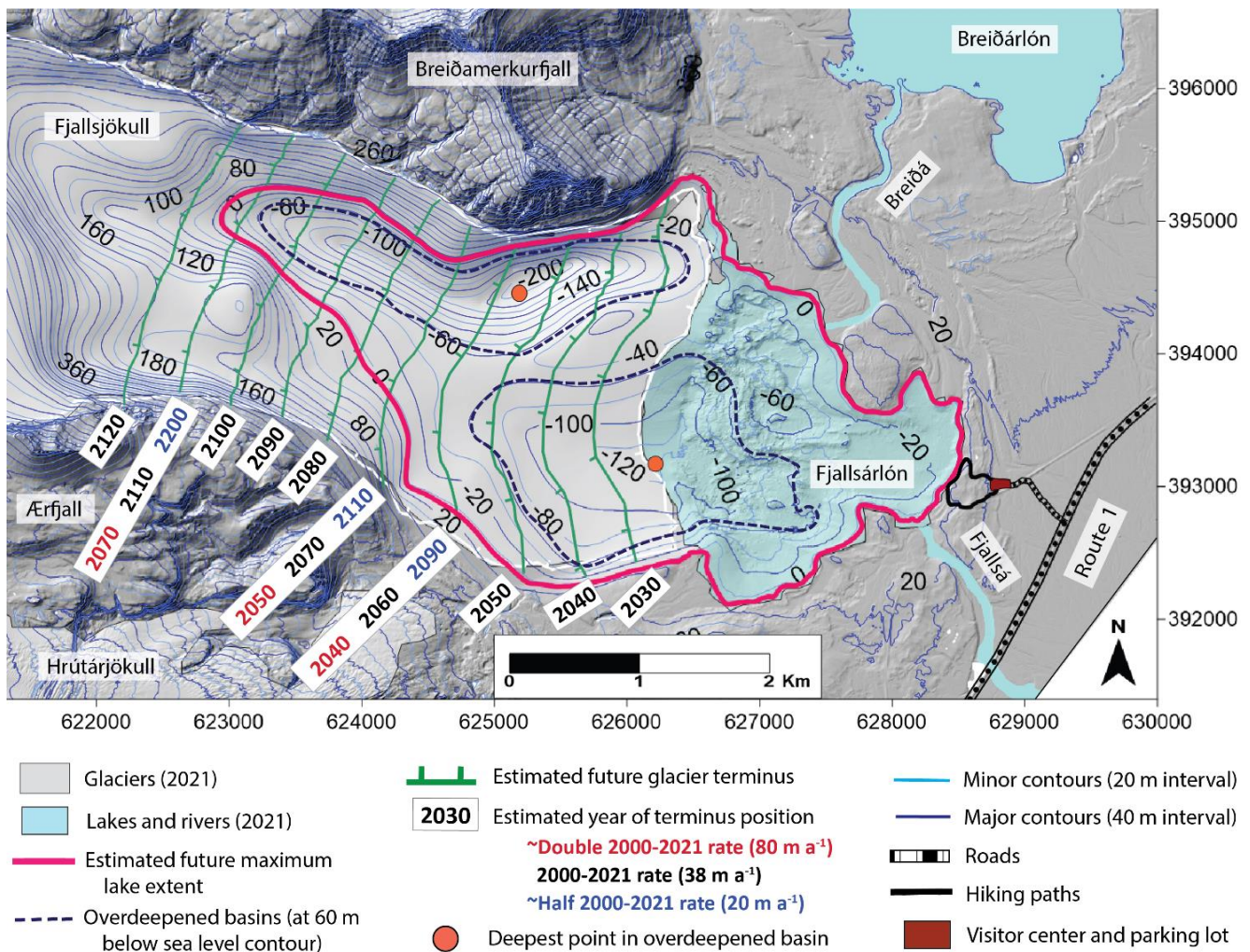


**Figure 4. Bed DEM showing overdeepened basins and estimated future development of Fjallsárlón extents and Fjallsjökull terminus positions from 2030–2120 for three terminus retreat rates, assuming linear rates and 2020 lake surface elevation (5 m a.s.l.). Bed DEM uses ISN93 coordinate system.**

#### 4.2. Glacier terminus change, 1890–2021

Fjallsjökull retreated 2.7 km from its Little Ice Age position in ~1890 to 2021, which averages to a rate of ~20 meters per year ( $\text{m a}^{-1}$ ). However, terminus retreat rates have varied significantly during different time intervals, averaging  $23 \text{ m a}^{-1}$  from 1890–1945,  $42 \text{ m a}^{-1}$  from 2000–2012,  $81 \text{ m a}^{-1}$  from 2012–2014, and  $11 \text{ m a}^{-1}$  from 2019–2021. The average annual terminus retreat rate from 2000–2021 was  $38 \pm 0.5 \text{ m a}^{-1}$  (Table 1). Terminus retreat horizontal uncertainties were derived from those reported by Hannesdóttir et al. (2020) for selected terminus positions (or, where our mapped terminus year did not correspond, uncertainties for the closest year). Calculated retreat depends on methodology and measurement location; for example, Hannesdóttir et al. (2015) reported 500 m of total retreat at Fjallsjökull from 1973–2010 based on a reference point on the land-terminating glacier, while Dell et al. (2019) calculated 870 m of retreat during the same time interval for the



glacier’s lake-terminating portion, with the faster rate attributed to mass loss through calving (Dell et al., 2019). For comparison, our method yields an intermediate value of ~700 m of retreat during a similar time period (1973–2012), which may be because it includes the entire glacier front (both land- and lake-terminating sections).

### 4.3. Lake surface area and volume changes, 1945–2021

Lake surface area and volume have increased since lake extent was first mapped in 1945 (Fig. 5). The 1945 lake had a surface area of  $0.33 \pm 0.01 \text{ km}^2$  and a volume of  $0.0055 \pm 0.0003 \text{ km}^3$ . By 2021, the lake covered  $3.65 \pm 0.05 \text{ km}^2$  and contained  $0.186 \pm 0.004 \text{ km}^3$  of water. Uncertainties were estimated by calculating surface areas and volumes for a lake surface elevation of 4 m a.s.l., and then calculating the corresponding uncertainty in lake area and volume relative to the current lake level (5 m a.s.l.) (an interval that fits within vertical uncertainties of  $<\pm 0.5 \text{ m}$  for sonar scanner bathymetry and lidar datasets). Surface area and volume increased during each successive time interval, with the exception of very slight decreases between 1985–1990 and 2016–2018 and no change between 1982–1983 and 1998–2000 (Fig. 5; Table 1). Past lake surface areas presented here are similar to those reported by Guðmundsson et al. (2019). Volumes also closely correspond to those calculated with other datasets, as differences between sonar scanner-derived volumes and volumes estimated from radio-echo sounding surveys and weighted rope point measurements for the 2018 lake are within calculated uncertainties (Guðmundsson et al., 2019).

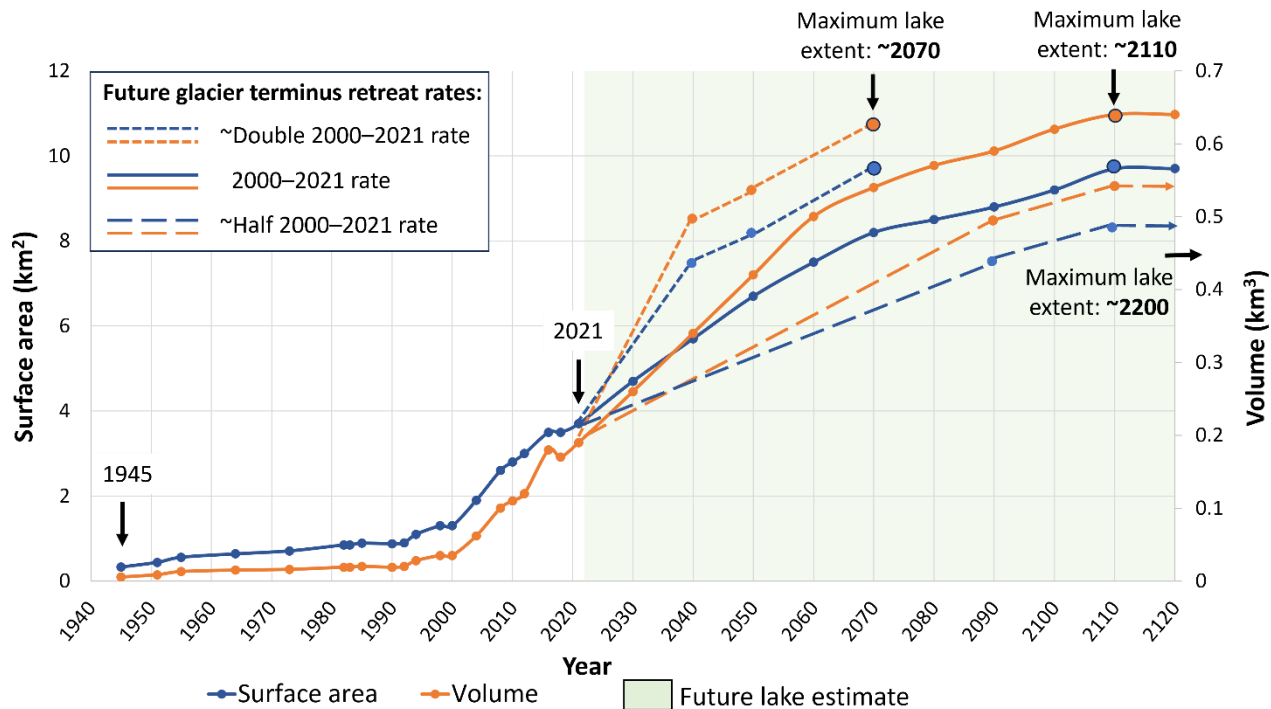


**Figure 5. Fjallsárlón surface area and volume at 20 time steps from 1945–2021 and projected evolution at decadal intervals from 2030–2120. Arrows denote timing of first mapped lake extent (1945), most recent measurement (2021), and estimated future maximum lake extents for three retreat rates (2070, 2110, and 2200).**

| Year                               | Lake surface area (km <sup>2</sup> ) <sup>a</sup>  | Lake volume (km <sup>3</sup> ) <sup>a</sup> | Maximum lake depth (m) <sup>b</sup> | Time interval for glacier change | Total glacier terminus retreat distance (m) within interval <sup>c</sup> | Average annual glacier terminus retreat rate (m a <sup>-1</sup> ) <sup>d</sup> |
|------------------------------------|--|---|-------------------------------------|----------------------------------|--|--|
| 1890                               | N/A  | N/A   | N/A                                 | 1890-1945                        | 1253 ± 30  | 23 ± 0.5   |
| 1945                               | 0.33 ± 0.01  | 0.0055 ± 0.0003                             | 32                                  | 1945-1973                        | 410 ± 20   | 15 ± 0.7   |
| 1951                               | 0.44 ± 0.01  | 0.0087 ± 0.0004                             | 37                                  |                                  |  |  |
| 1955                               | 0.56 ± 0.01  | 0.013 ± 0.001                               | 40                                  |                                  |  |  |
| 1964                               | 0.64 ± 0.01  | 0.015 ± 0.001                               | 42                                  |                                  |  |  |
| 1973                               | 0.71 ± 0.02  | 0.016 ± 0.001                               | 49                                  |                                  |  |  |
| 1982                               | 0.85 ± 0.02  | 0.019 ± 0.001                               | 43                                  | 1973-2000                        | 194 ± 15   | 7 ± 0.6  |
| 1983                               | 0.85 ± 0.02  | 0.019 ± 0.001                               | 43                                  |                                  |  |  |
| 1985                               | 0.89 ± 0.02  | 0.020 ± 0.001                               | 50                                  |                                  |  |  |
| 1990                               | 0.88 ± 0.02  | 0.019 ± 0.001                               | 44                                  |                                  |  |  |
| 1992                               | 0.90 ± 0.02  | 0.020 ± 0.001                               | 44                                  |                                  |  |  |
| 1994                               | 1.09 ± 0.02  | 0.028 ± 0.001                               | 62                                  |                                  |  |  |
| 1998                               | 1.28 ± 0.03  | 0.035 ± 0.001                               | 70                                  |                                  |  |  |
| 2000                               | 1.28 ± 0.03  | 0.035 ± 0.001                               | 70                                  |                                  |  |  |
| 2004                               | 1.91 ± 0.03  | 0.062 ± 0.002                               | 79                                  | 2000-2012                        | 509 ± 7  | 42 ± 0.6   |
| 2008                               | 2.64 ± 0.04  | 0.101 ± 0.003                               | 112                                 |                                  |  |  |
| 2010                               | 2.81 ± 0.05  | 0.112 ± 0.003                               | 119                                 |                                  |  |  |
| 2012                               | 2.98 ± 0.05  | 0.122 ± 0.003                               | 120                                 |                                  |  |  |
| 2016                               | 3.54 ± 0.05  | 0.177 ± 0.004                               | 128                                 | 2012-2014                        | 163 ± 4  | 81 ± 2   |
| 2018                               | 3.52 ± 0.05  | 0.173 ± 0.003                               | 126                                 | 2014-2017                        | 72 ± 4   | 24 ± 1   |
| 2021                               | 3.65 ± 0.05  | 0.186 ± 0.004                               | 128                                 | 2017-2019                        | 31 ± 4   | 15 ± 2   |
| 2030                               | 4.7 ± 0.9  | 0.26 ± 0.09                                 | 128                                 | 2019-2021                        | 21 ± 4   | 11 ± 2   |
| 2040                               | 5.7 ± 0.9  | 0.34 ± 0.11                                 | 146                                 | 2021-2030                        | 342 ± 5  | 38 ± 0.5   |
| 2050                               | 6.7 ± 0.9  | 0.42 ± 0.13                                 | 207                                 | 2030-2040                        | 380 ± 5  | 38 ± 0.5   |
| 2060                               | 7.5 ± 0.9  | 0.50 ± 0.14                                 | 210                                 | 2040-2050                        | 380 ± 5  | 38 ± 0.5   |
| 2070                               | 8.2 ± 1.0  | 0.54 ± 0.16                                 | 210                                 | 2050-2060                        | 380 ± 5  | 38 ± 0.5   |
| 2080                               | 8.5 ± 1.0  | 0.57 ± 0.16                                 | 210                                 | 2060-2070                        | 380 ± 5  | 38 ± 0.5   |
| 2090                               | 8.8 ± 1.1  | 0.59 ± 0.17                                 | 210                                 | 2070-2080                        | 380 ± 5  | 38 ± 0.5   |
| 2100                               | 9.2 ± 1.2  | 0.62 ± 0.17                                 | 210                                 | 2080-2090                        | 380 ± 5  | 38 ± 0.5   |
| 2110                               | 9.7 ± 1.5  | 0.64 ± 0.18                                 | 210                                 | 2090-2100                        | 380 ± 5  | 38 ± 0.5   |
| 2120                               | 9.7 ± 1.5  | 0.64 ± 0.18                                 | 210                                 | 2100-2110                        | 380 ± 5  | 38 ± 0.5   |
| Uncertainty estimation methodology |  |   |                                     |                                  |  |  |
|                                    | <sup>a</sup> <b>Lake surface area and volume:</b> differences between surface areas and volumes calculated for lake surface elevations at intervals corresponding to dataset vertical uncertainties. 1945–2021: lake surface elevations of 4 m and 5 m (sonar scanner bathymetry and lidar datasets have vertical uncertainties of ± < 0.5 m). 2030–2120: lake surface elevations of -15 m and 5 m (radio-echo sounding dataset has vertical uncertainty of ± 20 m). |   |                                     |                                  |  |  |
|                                    | <sup>b</sup> <b>Lake depth:</b> uncertainty for 1945–2021 is ± < 0.5 m (vertical uncertainty for sonar scanner bathymetry dataset); uncertainty for 2030–2120 is ± 20 m (vertical uncertainty for radio-echo sounding dataset).  |   |                                     |                                  |  |  |
|                                    | <sup>c</sup> <b>Total glacier terminus retreat:</b> extrapolated from horizontal uncertainties of glacier terminus positions for ~1890 (20 m); 1945 (10 m); 1982 (10 m); 2002 (5 m); and 2010 (2 m) (Hannesdóttir et al., 2020) by adding uncertainties of years within (or closest to) the time interval.   |   |                                     |                                  |  |  |
|                                    | <sup>d</sup> <b>Average annual glacier terminus retreat rate:</b> Uncertainty for total glacier terminus retreat rate averaged annually over time interval.  |   |                                     |                                  |  |  |

280 **Table 1. Past and estimated future development of Fjallsárlón and Fjallsjökull, showing lake surface area, volume, and maximum depth (below lake surface elevation of 5 m a.s.l.) at 20 time steps from 1945–2021; terminus retreat distance and average rate during nine time intervals from 1890–2021; and projected lake and glacier changes at decadal intervals from 2030–2120 (assuming linear continuation of 2000–2021 average annual terminus retreat rate of 38 m a<sup>-1</sup> and 2020 lake surface elevation of 5 m a.s.l.).**

#### 4.4. Future lake and glacier development

285 Assuming the lake will continue to expand westwards and maintain its 2020 surface elevation, a future lake will cover a maximum of  $9.7 \pm 1.5 \text{ km}^2$  and contain up to  $0.64 \pm 0.18 \text{ km}^3$  of water (Table 1; Fig. 5). This is quite similar to estimates of  $9.8 \text{ km}^2$  surface area and  $0.65 \text{ km}^3$  volume based on radio-echo sounding data (Magnússon et al., 2012). This estimated lake will fill both overdeepened troughs, with maximum depth almost doubling from 128 m to 210 m (Table 1; Fig. 4). Though there are small areas  $\sim 5 \text{ m a.s.l.}$  near the northern and southern lake shorelines, the rest of the basin is surrounded by higher-  
 290 elevation terrain and up to 25 m-high moraines, so the lake will likely only expand westward towards the retreating glacier terminus. Uncertainties were estimated by shifting the lake surface elevation vertically to -15 m below sea level, and then calculating the corresponding uncertainty in the lake area and volume relative to the current lake level (5 m a.s.l.) (matching the vertical uncertainties of  $\pm 20 \text{ m}$  of the radio-echo sounding dataset). Assuming that terminus retreat continues linearly into the future at the average 2000–2021 rate of  $38 \text{ m a}^{-1}$  and occurs at a uniform pace across the glacier front, Fjallsjökull's terminus  
 295 will become partially land-based after 2070. The lake-terminating section will progressively narrow as the lake expands into the northern overdeepening, with the glacier retreating into the deepest part of the lake around 2060 and completely withdrawing from the lake around 2110 (Fig. 4). If the glacier retreats at a rate approximately double that of 2000–2021 ( $80 \text{ m a}^{-1}$ ), the terminus will retreat into the deepest part of the lake around 2040, become partially land-based by  $\sim 2050$ , and exit the lake by  $\sim 2070$ . If the terminus retreats at a rate roughly half that of 2000–2021 ( $20 \text{ m a}^{-1}$ ), it will reach the deepest part of  
 300 the lake  $\sim 2090$ , become partially land-based around 2110, and withdraw from the lake by  $\sim 2200$  (Fig. 4).

#### 4.5. Mass movement potential and glacial lake outburst flood threat

Three sections of the valley walls above Fjallsjökull have slope angles  $>30^\circ$  with vertical relief  $>200 \text{ m}$ , giving them a high topographic potential to source large mass movements. These zones are located on slopes beneath the peaks of Miðaftanstindur and Eyðnatindur (part of Breiðamerkurfjall) and Ærfjallshöfuð (part of Ærfjall) (Fig. 6). Though the valley  
 305 walls have not been comprehensively geologically or structurally mapped, remote sensing and field observations reveal that they are primarily composed of rock with little or no overlying soil or sediment. No evidence of previous mass movements appears on Fjallsjökull in aerial photos (Landmælingar Íslands, 2022; Loftmyndir ehf., 2022).



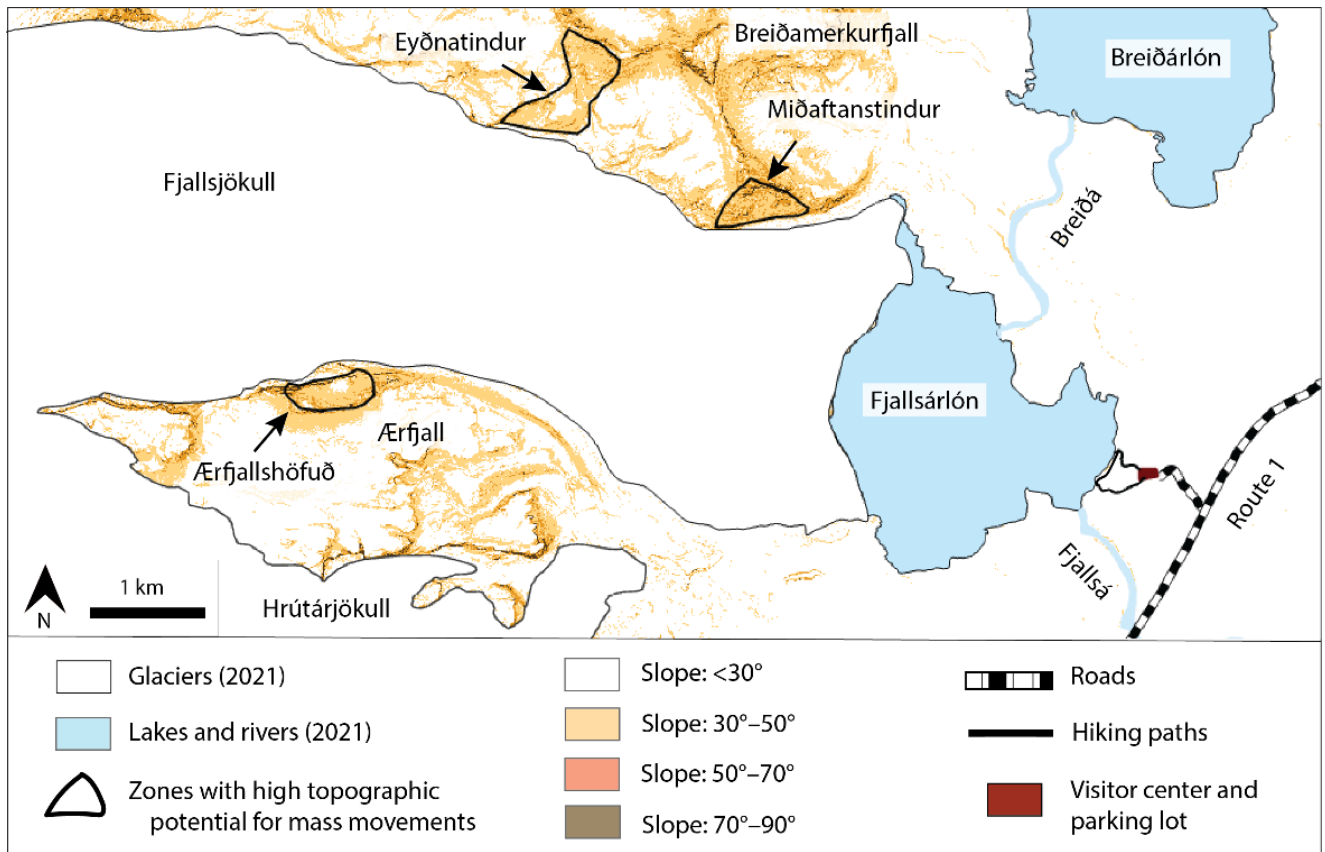


**Figure 6. Map of slope angles on subaerial terrain in study area based on 2021 glacier and lake extent. Delineated zones show areas in valley walls above Fjallsjökull with slope angles  $>30^\circ$  and vertical relief  $>200$  m, indicating high topographic potential to source large mass movements. ÍslandsDEM basemap with slope shading in ArcGIS Pro (Landmælingar Íslands, 2021).**

Miðaftanstindur, Eyðnatindur, and Ærfjallshöfuð are 1100 m, 3200 m, and 4500 m, respectively, from the 2021 glacier terminus, so a mass movement event would travel across the glacier surface to reach the lake (Table 2; Fig. 7). However, the zones of high topographic potential at Miðaftanstindur and Eyðnatindur extend beneath the 2021 glacier surface to the estimated future maximum lakeshore. As Fjallsjökull retreats, Miðaftanstindur will be situated directly above the lake, which could occur between ~2040 and 2090 based on the three estimated terminus retreat rates (Fig. 4). After the lake reaches its estimated maximum extent, a mass movement event from Eyðnatindur could also fall directly into the lake, while one from Ærfjallshöfuð would travel 1700 m to the lakeshore (Table 2; Fig. 7). Maximum vertical fall height for mass movement events from the three zones will increase as Fjallsjökull retreats. The highest point on Miðaftanstindur is 490 m above the 2021 glacier surface, an elevation that will increase to 600 m above the future lake surface. Maximum vertical fall heights for Eyðnatindur and Ærfjallshöfuð will increase from 520 m and 370 m above the 2021 glacier surface to 800 m and 870 m above the future lake surface, respectively. For a mass movement that enters the lake, the H/L ratio and angle of reach are highest for

325 Miðaftanstindur, followed by Eyðnatindur and Ærfjallshöfuð, and will increase in each zone as the glacier retreats and the lake expands. The H/L ratios range from 0.18–0.92, while angles of reach are between 10° and 43° (Table 2).

|  | Topographic parameter  | Zone  |   |   |
|--|--|---|---|---|
|  |  | Miðaftanstindur                                 | Eyðnatindur                                     | Ærfjallshöfuð                                   |
| 2021 glacier and lake positions                              | Maximum vertical height above glacier surface (m)                  | 490   | 520   | 370   |
|  | Horizontal distance from zone to glacier terminus (m)              | 1100  | 3200  | 4500  |
|  | H/L ratio and angle of reach (°) from zone to glacier terminus     | H = 600<br>L = 1600<br><b>H/L = 0.38</b><br>21° | H = 800<br>L = 4100<br><b>H/L = 0.20</b><br>11° | H = 870<br>L = 4900<br><b>H/L = 0.18</b><br>10° |
|  | Horizontal distance between highest and lowest zone boundaries (m) | 500   | 900   | 400   |
| Maximum future lake extent (after glacier retreat from lake) | Maximum vertical height above estimated future lake surface (m)    | 600   | 800   | 870   |
|  | Horizontal distance from zone to lakeshore (m)                     | 0   | 0   | 1700  |
|  | H/L ratio and angle of reach (°) from zone to lakeshore            | H = 600<br>L = 650<br><b>H/L = 0.92</b><br>43°  | H = 800<br>L = 1300<br><b>H/L = 0.62</b><br>32° | H = 870<br>L = 2100<br><b>H/L = 0.41</b><br>22° |
|  | Horizontal distance between highest and lowest zone boundaries (m) | 650   | 1300  | 400   |

330 **Table 2. Topographic parameters to assess potential for mass movements to enter Fjallsárlón from the three identified zones for 2021 glacier and lake positions and estimated maximum future lake extent after Fjallsjökull has retreated completely from the lake**

### 5. Discussion

#### 5.1. Lake bathymetry, volume, and evolution

335 The multibeam sonar survey provided a higher-resolution dataset for the bed DEM than was previously reported for Fjallsárlón from radio-echo sounding surveys and weighted rope point measurements, though volume differences between methods were within calculated uncertainties. This more detailed bathymetric map can be used for future studies on glacial erosional processes (i.e. overdeepening formation), depositional features (i.e. identifying subaqueous landforms), and the role of bathymetry in lake–terminus interactions (i.e. calving processes) (Purdie et al., 2016; Minowa et al., 2023).

Given the challenge of surveying glacial lakes in often remote and mountainous environments (Peng, 2023; Ramsankaran et al., 2023), many lake volumes are estimated with models based on ice thickness and proglacial and subglacial topography (Carrivick et al., 2022; Colonia et al., 2017; Frey et al., 2010; Grab et al., 2021; Linsbauer et al., 2016; Magnin et al., 2020; Otto et al., 2022). Other studies have applied area-related statistics or models to estimate lake volumes (Huggel et al., 2002; Loriaux and Cassassa, 2013; Cook and Quincey, 2015; Muñoz et al., 2020; Gantayat et al., 2024a). However, both models and equations are highly uncertain in estimating volume, especially in overdeepened basins (Cook and Quincey, 2015; Mölg et al., 2021; Kapitsa et al., 2023). Our bathymetric data offered an opportunity to test sonar scanner-derived volumes with a selection of empirical equations developed from lakes with similar sizes as Fjallsárlón (Table 3). Percent error between sonar scanner-derived volume and equation-predicted values varied from -13 to 16%, indicating fairly good agreement. However, this uncertainty also supports conclusions that equations do not accurately represent all glacial lake settings—particularly lakes such as Fjallsárlón that are in overdeepened basins and are not moraine- or ice-dammed. Our results illustrate the importance of directly measuring bathymetry to calculate volume and the need for more field-based datasets from overdeepened basins.

| Study                      | Equation<br>(V = volume; A = surface area)     | Calculated volume<br>(km <sup>3</sup> ) | Percent error (%)<br>(defined as: ((calculated volume–<br>measured volume)/(measured<br>volume)) * 100) |
|----------------------------|--|---|---|
| This study                 | Measured volume (from sonar<br>scanner survey) | 0.19                                    | N/A   |
| Cook and Quincey (2015)    | $V = 0.1746 * A^{1.3725}$                      | 0.18                                    | -4.7  |
| Huggel et al. (2002)       | $V = 0.104 * A^{1.42}$                         | 0.22                                    | 16  |
| Loriaux and Casassa (2013) | $V = 0.2933 * A^{1.3324}$                      | 0.16                                    | -13   |

**Table 3. Comparison of Fjallsárlón volume measured from sonar scanner survey with lake volumes predicted by selected empirical equations developed from lakes with similar sizes as Fjallsárlón.**

Sonar scanner surveys map the lake floor, not necessarily bedrock, and sediment thickness and sedimentation rate in Fjallsárlón are unknown and would require coring to determine. They may also have changed over time, adding uncertainty to calculated lake volumes. Sediment influx could also increase under future atmospheric warming due to greater subglacial meltwater runoff and erosion and/or supraglacial material sourced from mass movement events onto the glacier surface (Schomacker, 2010; Carrivick and Tweed, 2021; Ballantyne, 2022). Increased sediment input can decrease basin volume and thus lake storage capacity, so future lake volume estimates should be considered as maximum values (Magnin et al., 2020; Emmer et al., 2022; Steffen et al., 2022; Hosmann et al., 2024). Another unknown factor in future lake volume estimates is surface elevation of the Fjallsá river outlet (Purdie et al., 2016). However, Fjallsá base level is controlled by sea level, which is only 5 m below the current lake surface elevation—so while lake outlet geometry could lower via incision, this 5 m difference is captured in the uncertainty range of future volume estimates. If channel incision lowered lake surface elevation below 5 m

a.s.l., it is possible that warmer seawater could intrude tidally up the Fjallsá from the Atlantic Ocean, which could increase terminus melting rates. This may be occurring at Jökulsárlón, a proglacial lake at the nearby Breiðamerkurjökull glacier of Vatnajökull (Storarr et al., 2017).

## 5.2. Future glacier evolution and lake–terminus interactions

Many factors contribute to glacier retreat and advance rates, including climate, surface mass balance, ice velocity, subglacial topography, and lake–terminus interactions (Aðalgeirsdóttir et al., 2011; Cook and Swift, 2012; Dell et al., 2019; Jóhannesson et al., 2020). Estimating the future retreat rate can be done with an ice flow model coupled with a mass balance model at the outlet glacier scale. At Fjallsjökull, however, there is large uncertainty in climate projections, subglacial bedrock topography, and glacier dynamics. Therefore, applying a numerical model of future retreat will not provide more accurate results than the range of scenarios estimated by the three linear retreat rates. All three rates fall within the range of annual average terminus retreat observed at Fjallsjökull, with the fastest measured rate of  $81 \pm 2 \text{ m a}^{-1}$  from 2012–2014 and the slowest observed rate of  $7 \pm 0.6 \text{ m a}^{-1}$  from 1973–2000 (Table 1). Thus, future glacier terminus evolution should be considered as a first order estimate, though one based on recent observations that factors in the relative contributions of climate, subglacial topography, and lake–terminus interactions.

Numerous studies have projected future evolution of glaciers in Iceland, though results vary significantly depending on model spatial scale (global, Iceland, or ice cap), emission scenarios, and type of ice flow model. Nonetheless, all models project at least an 18% volume loss for Vatnajökull by 2100 (Schmidt et al., 2020; Compagno et al., 2021; Rounce et al., 2023). Projections for future climate conditions in Iceland indicate that deglaciation will not occur at a linear rate. Bosson et al. (2023) projected that glacier retreat will proceed at a similar rate globally until ~2040, then continue at different rates depending on emission scenarios. Noël et al. (2022) predicted an increase in glacier retreat rate after the mid-2050s under a high emission scenario due to the weakening of the Blue Blob, a region of cooling in the North Atlantic Ocean that has likely slowed down glacier retreat in Iceland since 2011. Thus, the only thing we can conclude with relative certainty is that Fjallsjökull will continue to retreat under a warming climate, and we use recently observed retreat rates to provide a first order estimate of future behavior.

In addition to climate scenarios and consequent surface mass balance, future glacier evolution is also controlled by meltwater runoff, subglacial water infiltration, calving, lake-induced melting at the terminus, and subglacial geothermal melting—which are not all captured in every model (Jóhannesson et al., 2020; Schmidt et al., 2020). Given this complexity, projecting volume change and retreat rate for Fjallsjökull specifically will require modelling at the individual outlet glacier scale. This has previously been done for another Vatnajökull outlet glacier, Hoffellsjökull, indicating a ~30% volume loss by 2100 (relative to its 2010 volume) if average climate conditions from 2000–2009 continue, with the glacier nearly disappearing by 2100 under projected temperature increases of  $1^{\circ}$ – $3^{\circ}\text{C}$  (Aðalgeirsdóttir et al., 2011). However, usual simplifications in dynamic ice flow models are not suited for the complex topography of Fjallsjökull due to its narrow outlet, steeply sloping bed, and relatively thin, highly crevassed ice flow over undulated bedrock.

Another factor in future glacier and lake evolution is lake–terminus interactions. When Fjallsjökull enters the northern overdeepened trough, maximum lake depth will nearly double from its deepest point in 2021. This will increase the surface area at the glacier front that is in contact with lake water, increasing melt. Deeper water will also increase torque and buoyancy forces at the terminus and thus calving rates. This, in turn, may reduce effective pressure and longitudinal stress, increasing ice flow and resulting in glacier thinning (Motyka et al., 2002; Benn et al., 2007; Dell et al., 2019; Baurley et al., 2020; Carrivick et al., 2020; Sutherland et al., 2020; Minowa et al., 2023). Increased lake depth and buoyancy force could also float the glacier tongue, eliminating basal friction at the glacial bed and increasing ice flow velocity and thus thinning, crevassing, and ice disintegration (Motyka et al., 2002; Benn et al., 2007; Boyce et al., 2007; Baurley et al., 2020; Main et al., 2022). Terminus flotation has occurred at Heinabergsjökull and Hoffellsjökull, other Vatnajökull outlet glaciers (Aðalgeirsdóttir et al., 2011; Guðmundsson et al., 2019). Though some parameters to calculate future terminus calving rate and flotation potential are known (lake bathymetry, water density, and ice density), others are not (glacier velocity, ice thickness, ice terminus height above buoyancy, and subaqueous melt rates) (Brown et al., 1982; Benn et al., 2007; Carrivick et al., 2020; Vieli, 2021; Main et al., 2022; Minowa et al., 2023). Studies at other global lake-terminating glaciers have used models to estimate future glacier retreat rates, lake development, and calving rates (i.e. Gantayat et al., 2024b); however, given the limited data availability, glacier and topographic complexity, and process and boundary condition uncertainty at Fjallsjökull, these modelling approaches would not yield significantly accurate results to advance our conclusions.

Even if calving rates increase, the lake-terminating glacier front will become narrower as Fjallsjökull retreats into the northern overdeepening, potentially reducing the amount of mass loss through calving (Fig. 4). In 2021, the terminus calving front was 2.7 km wide. Assuming the glacier retreats at the estimated 2000–2021 rate, the calving front will span ~2 km around 2050 and ~1 km around 2080. Moreover, retreat rates will likely vary across the terminus, resulting in different configurations than the estimated simple straight line shapes (Fig. 4). Part of the terminus is projected to become land-based between ~2050 and ~2110 (depending on the retreat scenario), which may retreat at a different rate than the lake-terminating front; though our calculated average annual retreat rates include both lake- and land-terminating sections, which may capture these differences (Fig. 4).

Considering all factors, we can conclude with relative certainty that Fjallsjökull’s retreat rate will likely increase after the middle of the 21<sup>st</sup> century due to rising atmospheric temperatures and increased calving and subaqueous melting as the terminus retreats into the northern overdeepening. Retreat is unlikely to be linear over time and across the glacier terminus due to changing climate conditions, subglacial topography, and geometry of the lake-terminating glacier front. Though the exact timeline of glacier retreat is uncertain, the three estimated rates indicate that Fjallsjökull will retreat into the deepest part of the lake within the next several decades, and the lake will reach its maximum extent within the next one to two centuries.

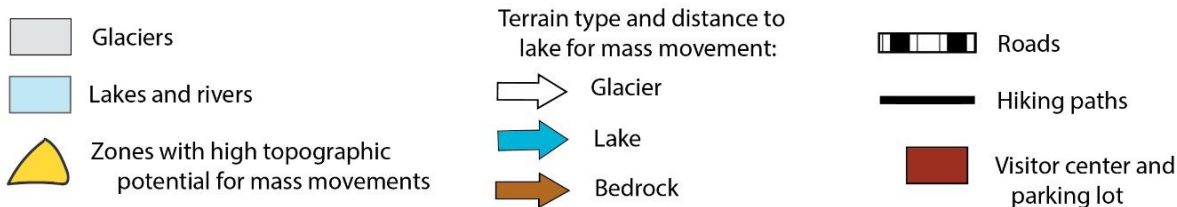
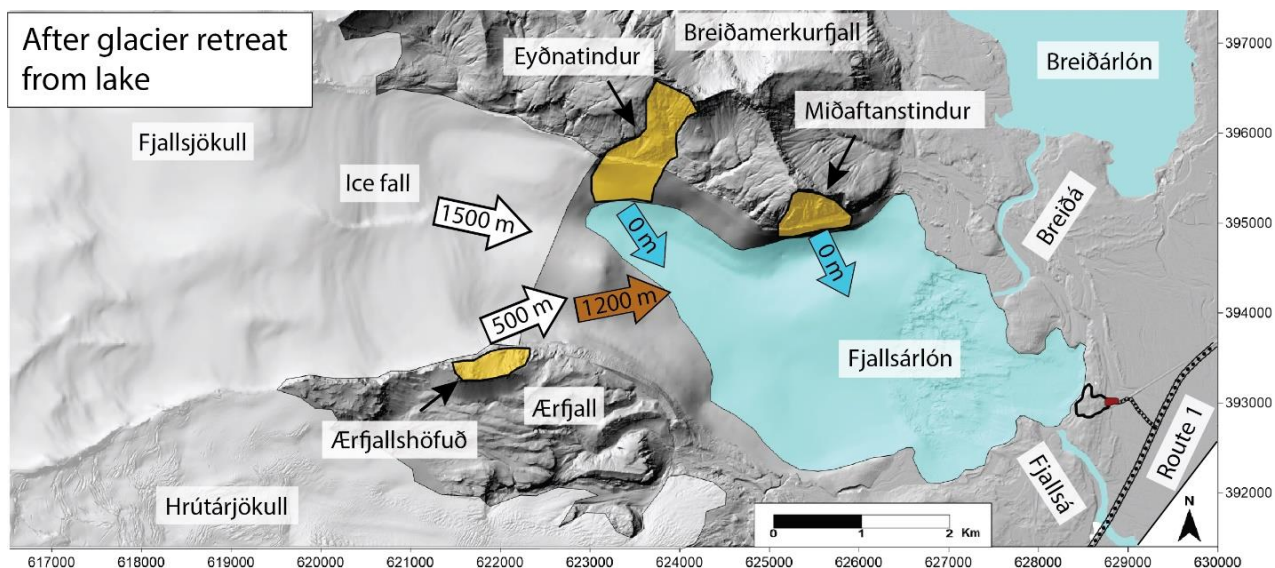
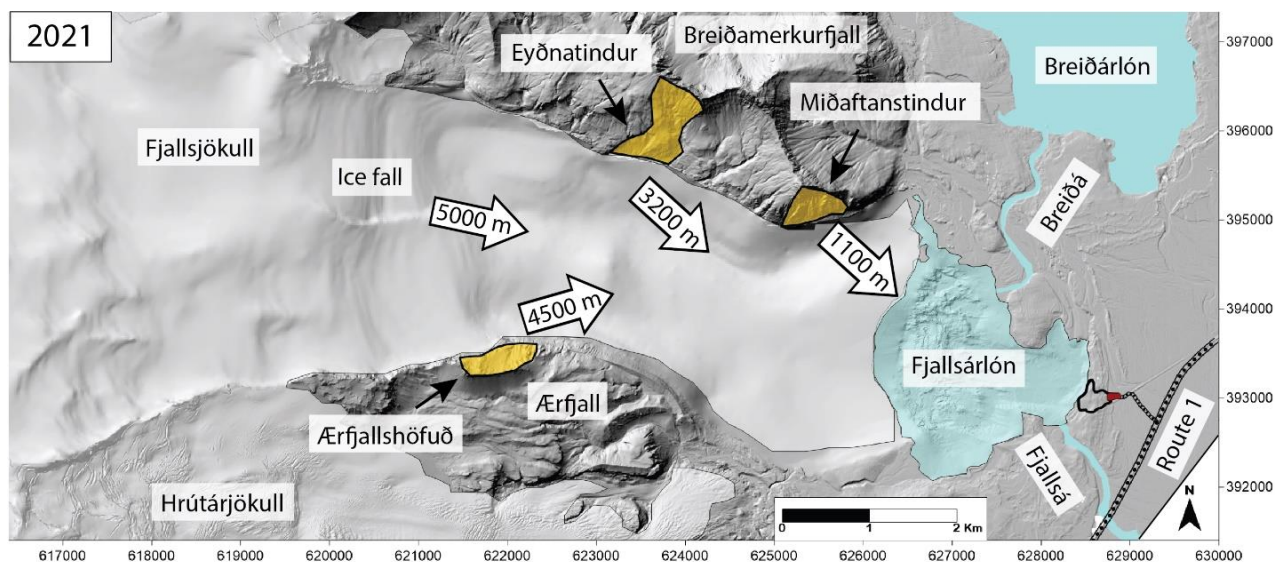
### 5.3. Mass movement scenarios into Fjallsárlón

Three zones of the valley walls above Fjallsjökull have a high topographic potential of sourcing large mass movements, though we cannot predict the exact location, volume, or failure plane of an event without comprehensive

430 geological and structural mapping (McColl, 2012; Hartmeyer et al., 2020). Geological mapping in necessary detail has not been done for the valley walls above Fjallsjökull; and studies from other Öraefajökull outlet glaciers indicate that regional geology is too complex to interpret solely from remote sensing data such as drone or satellite imagery (Helgason and Duncan, 2001; Ben-Yehoshua et al., 2023). However, future geological field mapping could identify structural weaknesses such as fractures and faults that might be gravitationally activated under ice thinning or disappearance (Kos et al., 2016; Higman et al., 2018). This would help map potential failure planes and estimate landslide volumes and source locations. Additionally, methods such as InSAR or DEM differencing could identify areas of deformation on the valley walls, as has been done in Iceland (Lacroix et al., 2022; Ben-Yehoshua et al., 2023), Greenland (Svennevig et al., 2020), Switzerland (Kos et al., 2016), Norway (Hermanns et al., 2013), Alaska (Higman et al., 2018), and Canada (Geertsema et al., 2022), for example.

Given the current level of knowledge, our results reveal several possible scenarios for mass movements to enter Fjallsárlón and generate displacement waves or GLOFs (Fig. 7). Given the predominant rock composition of the valley walls, a mass movement event will likely be a rock slope failure such as a rock fall (with a volume lower than the threshold for material to flow, causing most material to be deposited near the failure slope) or rock avalanche (with a volume exceeding the threshold for flow, enabling material to travel away from the source area), with the classification determined by the vertical fall height (H), horizontal travel distance (L), and angle of reach (Evans et al., 2006; Hungr et al., 2014; Hermanns et al., 2022). At the estimated future maximum lake extent, the H/L ratio and angle of reach at Miðaftanstindur will exceed the thresholds of 0.625 and 32°, respectively, meaning that a rock fall would enter the lake. For all other scenarios (from all three zones in 2021 and Eyðnatindur and Ærfjallshöfuð at future maximum lake extent), H/L ratios are <0.625 and angles of reach are ≤32°, so mass movements must have large enough volumes to classify as rock avalanches in order to reach the lake.

450



455 **Figure 7. Scenarios of mass movements entering Fjallsárlón based on glacier and lake positions in 2021 and at the estimated maximum lake extent after Fjallsjökull has retreated completely from the lake. Bed DEM basemap with ISN93 coordinate system.**



Several factors control mass movement mobility and runout distance and thus whether material will reach Fjallsárlón. Material traveling across a glacier will have high mobility due to low friction on the glacier surface and frictional melting of ice, resulting in a greater runout distance (Sosio et al., 2012; De Blasio, 2014; Deline et al., 2022). Fjallsjökull's surface gradient in 2021 was approximately 6° along the central flow line for the section down-valley of the three identified zones. There are numerous global precedents of rock avalanches onto glaciers with similar gradients and angles of reach where runout distances have exceeded 4500 m, the longest horizontal distance in our scenarios (Sosio et al., 2012; Delaney and Evans, 2014; Sosio, 2015; Hermanns et al., 2015; Aaron and McDougall, 2019; Ben-Yehoshua et al., 2022; Deline et al., 2022). Increased water content can also increase rock fall or rock avalanche mobility and thus runout distance. If a failure plane extends from the valley wall under the glacier, a mass movement event could fracture the glacier and incorporate glacial ice, increasing mobility by reducing friction between clasts and adding meltwater to the material (Sosio et al., 2012; Deline et al., 2022). This could occur at Fjallsjökull since the high topographic potential zones at Miðaftanstindur and Eyðnatindur extend beneath the 2021 glacier surface (Fig. 7). Additionally, the large maximum vertical fall heights at all three zones mean that a rock fall or rock avalanche may transfer enough energy to fracture or melt the glacier, incorporating ice blocks and water (Byers et al., 2019; Shugar et al., 2021). Vertical fall heights (and thus potential energy transfer) will increase with projected glacier thinning—though this mass loss will also reduce the ice volume available to fracture or melt. Given these potential interactions with the glacier, it is possible that a rock fall onto Fjallsjökull could become mobile enough to transform into a rock avalanche and travel down the glacier to enter the lake. Studies at other sites have modelled rock fall or rock avalanche propagation dynamics, but these models require input data such as slope failure release area and mass movement volume, which we cannot estimate at Fjallsjökull without detailed geological mapping (Sosio et al., 2012; Delaney and Evans, 2014; Cathala et al., 2024).

Out of all scenarios, a mass movement from Miðaftanstindur may pose the greatest GLOF threat since the lake is projected to expand beneath the entire mountain in the next few to several decades, and even a smaller event such as a rock fall will enter the lake, resulting in direct energy transfer to the lake rather than attenuation during impact and travel across the glacier. A rock fall from Eyðnatindur could directly enter the lake, as well, but this would not occur until the lake reached its estimated maximum extent. For all other scenarios, GLOF threat will also likely increase with future projected Fjallsjökull terminus retreat. With all other factors remaining equal, decreased horizontal travel distances between high topographic potential zones and the lake indicate that: 1) a rock avalanche with a smaller volume will be able to reach the lake; and 2) a rock avalanche will lose less energy along its shorter travel path and transfer more material to the lake to generate larger displacement waves. However, terrain type along the rock avalanche travel path will also change as the terminus retreats, potentially reducing this increased GLOF threat. At the estimated maximum lake extent, a rock avalanche from Ærfjallshöfuð will travel 500 m across the glacier surface and 1200 m across bedrock terrain, which will increase surface friction and eliminate interactions with ice, reducing material mobility and runout distance (Fig. 7). Finally, it is important to note that while three identified zones have high topographic potential of sourcing mass movements, slope failures could occur from other locations in the valley walls due to structural weaknesses such as faults or fractures or a high degree of weathering.

Moreover, GLOF threat from Fjallsárlón will likely persist after Fjallsjökull retreats from the lake basin since glacial meltwater will continue to drain into the lake, and valley walls will continue to experience paraglacial instability.

495 A mass movement from the valley walls above Fjallsjökull could be triggered by numerous processes. First, Fjallsjökull is an outlet glacier of Öräfajökull, which is an active volcano that experiences periodic seismic activity that could potentially generate a rock slope failure (Keefer, 1984; Einarsson, 2019). Second, extreme precipitation events could trigger rock slope failures by increasing pore water pressure and adding weight to slopes (Chigira, 2009; Chigira et al., 2013). This process triggered a landslide in 2013 onto Svínafellsjökull, another Öräfajökull outlet glacier, that traveled nearly 4 km down the glacier surface (Ben-Yehoshua et al., 2022). Third, continued glacier retreat and thinning will expose new valley wall sections to paraglacial processes such as debuitressing, freeze-thaw activity, and crustal rebound stress adjustments, which could destabilize rock and result in rock falls or rock avalanches (Dai et al., 2020). However, one common paraglacial trigger of mass movements in other environments that is likely not a factor at Fjallsjökull is permafrost thaw (Haeberli et al., 2017; Hilger et al., 2018). Estimated permafrost distribution in Iceland is mostly in the northern and central highland regions and above 800–1000 m a.s.l. (Etzel Müller et al., 2007, 2020; Czekirda et al., 2019). Back-calculated ground temperatures on valley walls above Svínafellsjökull, which has a similar climatic setting to Fjallsjökull, indicate that permafrost conditions have not occurred below 1000 m a.s.l. since ~1900 (Ben-Yehoshua et al., 2022).

Ice avalanches may also pose a threat of triggering a GLOF at Fjallsárlón, as they do at other glacial lakes worldwide (Kershaw et al., 2005; Frey et al., 2010; Schaub et al., 2016; Geertsema et al., 2022; Tang et al., 2023). Ice avalanches can fall from steep glacier sections or result from changes in glacier dynamics, such as ice velocity increases, deeper or more spatially extensive crevassing, or changes in glacier hydrology or geometry that alter ice stresses and decrease basal friction at the bed (Evans and Clague, 1994; Deline et al., 2021). An ice fall occurs ~5 km from the 2021 terminus where the glacier flows over bedrock steps—a distance that will shorten to ~1.5 km when the lake expands to its projected future maximum extent (Fig. 7). Glacier stress dynamics in this ice fall may change as atmospheric temperatures increase and the terminus enters deeper water. Additionally, large calving events from the glacier terminus may generate displacement waves in Fjallsárlón (Cook et al., 2016).

515 Finally, even if a rock avalanche occurs from the slopes above Fjallsjökull and does not continue into the lake, it could influence future glacier dynamics by insulating the surface to slow melting (with thicker debris cover), increasing ablation to enhance melting (with thinner debris cover), changing glacier velocity or sediment transport, or depositing material on the glacier surface for mobilization by another rock avalanche (Haritashya et al., 2018; Bessette-Kirton and Coe, 2020; Deline et al., 2022). Thus, projecting the location and dynamics of potential mass movements onto Fjallsjökull is important even if they do not enter Fjallsárlón.

#### 5.4. Glacial lake outburst flood threat and potential impacts

Even if a rock fall, rock avalanche, or ice avalanche enters Fjallsárlón, it will not necessarily generate a displacement wave, and it will only trigger a GLOF downstream if waves exit the lake basin. Numerous factors control displacement wave propagation dynamics, runup height, and whether the wave travels as a single wave or seiche wave (repeated waves in the basin). Though we have some required input datasets (lake bathymetry, shoreline geometry, and subaerial topography of the lakeshore area), other parameters are uncertain without accurate estimates of mass movement volume or source area (material velocity, volume, frontal area, and lake entry angle and location) (Romstad et al., 2009; Harbitz et al., 2014; Westoby et al., 2014a; Oppikofer et al., 2018). Given the current level of knowledge, we cannot accurately predict displacement wave behavior—only impacts of potential runup wave scenarios.

Though Fjallsárlón is not moraine-dammed, moraines surround most of its shoreline. Displacement waves exceeding ~25 m high would overtop the tallest moraines, potentially continuing as a GLOF downstream. Waves could also incise the moraines to create a lower-elevation breach for subsequent, smaller waves to exit (Hubbard et al., 2005; Evans et al., 2006; Emmer and Vilímek, 2013; Westoby et al., 2014a). Displacement waves of any height could exit the lake via the Fjallsá outlet, which forms a topographic low point along the shoreline. If a mass movement enters Fjallsárlón, the greatest distance for displacement waves to travel between any points along the 2021 lake shoreline is ~2.5 km, which will increase to ~6 km at estimated future maximum lake extent. Mass movement-triggered displacement waves have exceeded 25 m high and traveled more than 6 km at lakes with similar sizes to Fjallsárlón, including in Iceland (Gylfadóttir et al., 2017) and Canada (Roberts et al., 2013), indicating that (though dependent on mass movement characteristics) waves could realistically exit the Fjallsárlón basin and drain in a GLOF.

A displacement wave or GLOF at Fjallsárlón could have a significant societal impact. If overtopping or breaching occurs at the moraines on the eastern lakeshore, floodwaters could inundate a visitor center and parking lot approximately 300 m downstream, as well as hiking paths in between. A displacement wave with a runup height of even 1 m could impact people at the shoreline, which is a popular viewpoint and the launch site for boat tours on Fjallsárlón. If a wave surged through the lake outlet to drain along the Fjallsá river, it would travel only ~1 km before reaching a bridge along Route 1 (Fig. 8). This is Iceland's main road and the only land transport and supply connection between east and west Iceland on the south coast, so damage to the road or bridge could have significant economic and tourism impacts not just at Fjallsjökull but at a regional scale (Welling et al., 2020; Welling and Abegg, 2021). Moreover, these infrastructure and visitor sites are concentrated on the eastern edge of the lake, which is roughly perpendicular to the direction from which a mass movement from any of the three identified zones would enter Fjallsárlón, and displacement waves tend to be highest when they approach perpendicular to a location (Frey et al., 2018; Hermanns et al., 2022).

A GLOF from Fjallsárlón would also significantly impact the landscape. Based on Fjallsjökull's proglacial geomorphology and impacts observed in similar depositional settings, an outburst flood would likely erode channels in sediment (including enlarging the Fjallsá outlet), transport moraine and sandur material, and deposit boulders, gravel bars, and/or sediment fans (Kershaw et al., 2005; Russell et al., 2006; Wilson et al., 2019; Chandler et al., 2020; Wells et al., 2022).

This material redistribution could damage or destroy roads, trails, the bridge, the parking lot, and the tourist center, leaving a long-term geomorphologic legacy after floodwaters receded (Fig. 8).

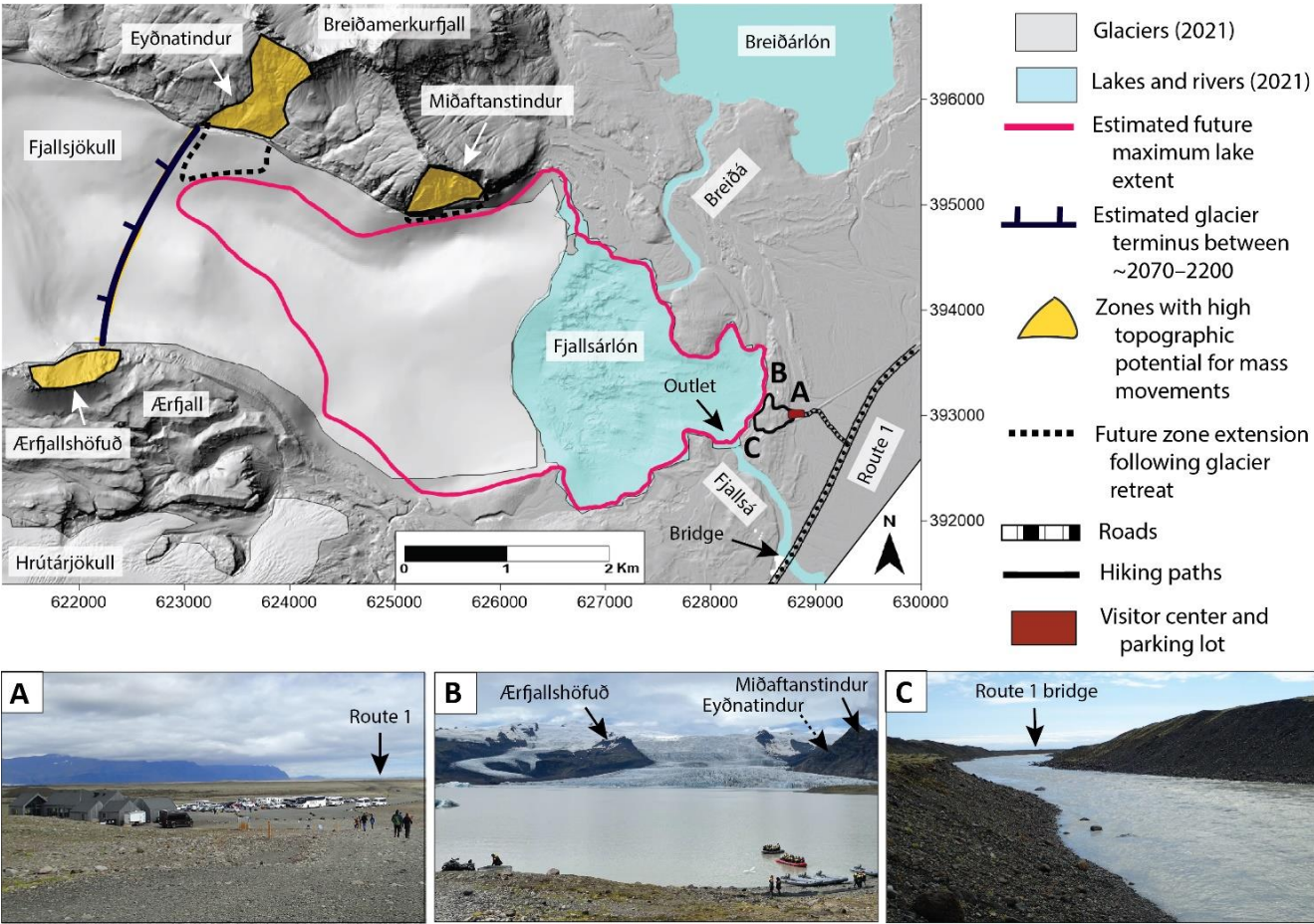


**Figure 8. Map illustrating potential societal and landscape impacts of mass movement-triggered displacement waves or GLOFs in Fjallsárlón. Bed DEM basemap with ISN93 coordinate system. Photos A–C correspond to locations marked on the map: (A) View looking northeast towards the visitor center, parking lot, and Route 1. (B) View looking west towards Fjallsjökull showing hiking trails and boat launches along the lakeshore, with high topographic potential zones marked. (C) View looking southeast along the Fjallsá outlet towards the Route 1 bridge.**

### 5.5. Future research directions and broader implications

Though a comprehensive risk and hazard assessment is beyond the scope of this study, our results provide information that can contribute to developing one. Lake bathymetry is a crucial input dataset for modelling displacement wave propagation and dam breach scenarios (Harbitz et al., 2014; Worni et al., 2014; Haritashya et al., 2018; Lala et al., 2018; Mergili et al., 2020; Sattar et al., 2021, 2023; ; Rinzin et al., 2023). High-resolution multibeam sonar measurements of bathymetry can also be used to test and calibrate models that estimate overdeepening volumes (Cook and Quincey, 2015). Additionally, lake extent,

volume, and proglacial topography serve as inputs for numerical hydraulic modelling to simulate flood routes, depths, and peak discharges for different lake drainage scenarios, as has been done for lakes in the Himalayas, for example (Worni et al., 2013; Somos-Valenzuela et al., 2015; Allen et al., 2022b; Sattar et al., 2023). This can help predict geomorphologic impacts—for example, zones of erosion versus deposition and the type of material transported—to prepare for repair and clean-up efforts, as well as inform engineering solutions for flood mitigation (Westoby et al., 2014b; Allen et al., 2022b; Geertsema et al., 2022). Finally, this study identifies three zones with high topographic potential of mass movements to prioritize for geological and structural mapping and monitoring, perhaps following approaches at unstable slopes at other sites worldwide (Purdie et al., 2015; Kos et al., 2016; Hartmeyer et al., 2020; Svennevig et al., 2020; Lacroix et al., 2022; Ben-Yehoshua et al., 2023; Moragues et al., 2024). Taken together, this research can help local and national authorities to develop risk assessments, plan future infrastructure and tourism access, and communicate this new, emerging hazard to locals and visitors (Stewart et al., 2016; Frey et al., 2018; Strzelecki and Jaskólski, 2020; Matti and Ögmundardóttir, 2021; Welling and Abegg, 2021; Allen et al., 2022a; Matti et al., 2023).

This study's methodology can also be applied to other proglacial areas where glacier retreat, lake expansion, and growth of potential GLOF societal impact is outpacing the speed of research. Other cryospheric risk assessment methodologies exist, such as GAPHAZ (2017), which numerous studies have successfully applied (Allen et al., 2022b; Rinzin et al., 2023; Sattar et al., 2023). However, some sites lack the necessary input data for comprehensive risk analyses, so initial assessments are useful for prioritizing areas for monitoring and additional data collection. This approach is ideal for places where mass movement-triggered GLOFs have not yet become a frequent hazard but are likely to in future. One such region is the south coast of Iceland, which features over a dozen outlet glaciers with expanding proglacial lakes and increasing numbers of visitors (Guðmundsson et al., 2019; Welling and Abegg, 2021; Welling et al., 2020). However, only one site, Svínafellsjökull, has acted to mitigate this risk. Since a rock avalanche occurred on the glacier in 2013, fractures and slope deformation have been mapped and monitored on the valley walls, and authorities have held informational meetings with the local community and cancelled tourist activities on the glacier (Matti and Ögmundardóttir, 2021; Ben-Yehoshua et al., 2022). This approach is also suitable for other Arctic and subarctic regions where mass movement-triggered GLOFs or tsunamis have only recently emerged as hazards amidst increasing tourism, infrastructure development, or shipping traffic, such as Greenland (Strzelecki and Jaskólski, 2020; Svennevig et al., 2020, 2024; Matti et al., 2023), Alaska (Wieczorek et al., 2007; Higman et al., 2018; Dai et al., 2020), and Arctic Canada (Matthew et al., 2024).

## 6. Conclusions

Fjallsárlón has significantly expanded since it was first mapped in 1945, increasing in surface area by  $\sim 3.3 \text{ km}^2$  and in volume by  $\sim 0.18 \text{ km}^3$  to cover  $3.65 \pm 0.05 \text{ km}^2$  and contain  $0.186 \pm 0.004 \text{ km}^3$  of water by 2021. Over the same time interval, measured maximum water depth increased from 32 m to 128 m as the lake expanded into an overdeepened basin. Lake volumes calculated from multibeam sonar measurements of bathymetry generally match those estimated from radio-echo sounding

surveys and weighted rope point measurements, indicating good agreement between methods. However, differences are greater when sonar scanner-derived volumes are compared with those calculated from empirical equations, supporting calls for more field measurements to refine equations, especially from lakes in overdeepened basins.

If Fjallsárlón maintains its 2020 surface elevation, the lake will reach a maximum surface area of  $9.7 \pm 1.5 \text{ km}^2$  and volume of  $0.64 \pm 0.18 \text{ km}^3$ , fill the rest of the southern overdeepened basin, and occupy the northern trough, increasing its maximum depth to  $\sim 210 \text{ m}$ . Regional-scale glacier evolution models indicate that Vatnajökull will continue to lose mass under all emission scenarios (Schmidt et al., 2020; Compagno et al., 2021; Rounce et al., 2023), with atmospheric temperatures likely increasing at a faster rate after the mid-21<sup>st</sup> century (Noël et al., 2022). However, given uncertainty and complexity in climate projections, subglacial bedrock topography, and glacier dynamics, a numerical model of retreat at the outlet glacier scale will not provide more accurate results than a range of linear retreat rates based on recent observations. Applying these three rates indicates that Fjallsjökull will retreat into the deepest part of the northern overdeepening within the next few to several decades. This will likely increase ice loss due to greater calving rates and subaqueous melting, which—along with projected atmospheric temperature rise—will increase ice thinning and velocity and potentially cause flotation of the glacier tongue. The glacier will likely retreat completely out of the lake within the next one to two centuries. However, numerous factors control future glacier and lake development; thus, these scenarios should be considered as a first order estimate rather than a realistic timeline for retreat.

Three zones on the valley walls above Fjallsjökull have a high topographic potential for sourcing mass movements due to slope angles  $>30^\circ$  and vertical relief  $>200 \text{ m}$ : the slopes beneath Miðaftanstindur, Eyðnatindur, and Ærfjallshöfuð. Based on 2021 lake extent, a rock avalanche from these zones would travel between  $\sim 1100 \text{ m}$  and  $\sim 4500 \text{ m}$  before entering Fjallsárlón, which is realistic given increased mobility from reduced friction of the ice surface and likely incorporation of meltwater. A mass movement from Miðaftanstindur poses the greatest threat of triggering a GLOF since it is situated closest to Fjallsárlón, and a rock fall or rock avalanche could directly enter the lake in the next few to several decades. GLOF threat will also likely increase from Eyðnatindur and Ærfjallshöfuð as Fjallsjökull retreats, with rock avalanche travel distance to the lake decreasing to a minimum of  $0 \text{ m}$  and  $\sim 1700 \text{ m}$ , respectively, at estimated maximum lake extent. However, material will flow over higher-friction bedrock terrain, potentially reducing runout distance.

If a rock fall, rock avalanche, or ice avalanche enters Fjallsárlón, displacement waves with runup heights as low as  $1 \text{ m}$  could impact visitors and boats on the shoreline. If runup heights exceed  $\sim 25 \text{ m}$ , waves could overtop and/or incise the highest moraines on the lake's eastern shore, inundating the tourist center and parking lot  $\sim 300 \text{ m}$  downstream. Displacement waves could also exit the lake through the Fjallsá river outlet and continue as a GLOF  $\sim 1 \text{ km}$  to the Route 1 road and bridge. These scenarios could significantly impact human security, infrastructure, and transportation connections, with societal and economic effects extending throughout the region. A GLOF would also erode and redistribute large quantities of sediment and moraine material, leaving a long-term geomorphologic legacy.

Mass movement-triggered GLOFs will likely pose a greater threat at other proglacial lakes in Iceland and Arctic and alpine regions worldwide with ongoing climate change. Directly measuring lake bathymetry, quantifying past lake change,

and projecting future lake evolution are crucial for understanding how glaciers, hydrology, and landscapes interact and respond to these conditions. Results also provide crucial input datasets for additional studies on lake–terminus interactions, displacement wave propagation, and risk mitigation strategies. Assessments such as this are especially useful for regions like south Iceland and other Arctic and subarctic sites where mass movement-triggered GLOFs have not frequently occurred but are an emerging hazard due to rapid environmental change and increased visitor numbers and infrastructure development. This approach can help select priority areas for monitoring and additional data collection, with the goal of mitigating GLOF impact even if detailed site studies have not been completed.

**Author contribution**

GHW prepared the manuscript with review and editing by all co-authors. GHW and ÞS conceptualized the project. FP and EM provided radio-echo sounding data. ÞS collected sonar scanner bathymetric data. SG provided glacial lake outlines from 1945–2018.

**Competing interests**

The authors declare that they have no conflict of interest.

**Acknowledgements**

This project was completed as part of a University of Iceland Post-doc Grant to GHW. The multibeam sonar scanner bathymetric survey of Fjallsárlón in 2020 was conducted by Köfunarþjónustan and funded by a grant to ÞS from the Landsvirkjun Energy Research Fund (Orkurannsóknasjóður Landsvirkjunar, received in 2019).

**References**

Aaron, J. and McDougall, S.: Rock avalanche mobility: The role of path material, *Eng. Geol.*, 257, 105126, <https://doi.org/10.1016/j.enggeo.2019.05.003>, 2019.

Aðalgeirsdóttir, G., Guðmundsson, S., Björnsson, H., Pálsson, F., Jóhannesson, T., Hannesdóttir, H., Sigurðsson, S.P., and Berthier, E.: Modelling the 20th and 21st century evolution of Hoffellsjökull glacier, SE-Vatnajökull, Iceland, *Cryosphere*, 5, 961–975, <https://doi.org/10.5194/tc-5-961-2011>, 2011.

Aðalgeirsdóttir, G., Magnússon, E., Pálsson, F., Thorsteinsson, T., Belart, J.M.C., Jóhannesson, T., Hannesdóttir, H., Sigurðsson, O., Gunnarsson, A., Einarsson, B., Berthier, E., Schmidt, L.S., Haraldsson, H.H., and Björnsson, H., Glacier changes in Iceland from ~1890 to 2019, *Front. Earth Sci.*, 8, 574754, <https://doi.org/10.3389/feart.2020.523646>, 2020.

Allen, S.K., Zhang, G., Wang, W., Yao, T., and Bolch, T.: Potentially dangerous glacial lakes across the Tibetan Plateau revealed using a large-scale automated assessment approach, *Sci. Bull.*, 64, 435–445, <https://doi.org/10.1016/j.scib.2019.03.011>, 2019.

Allen, S., Frey, H., Haeberli, W., Huggel, C., Chiarle, M. and Geertsema, M., Assessment principles for glacier and permafrost



hazards in mountain regions, Oxford Research Encyclopedia of Natural Hazard Science, doi.org/10.1093/acrefore/9780199389407.013.356, 2022a.

- 675 Allen, S.K., Sattar, A., King, O., Zhang, G., Bhattacharya, A., Yao, T., and Bolch, T.: Glacial lake outburst flood hazard under current and future conditions: Worst-case scenarios in a transboundary Himalayan basin, *Nat. Hazards Earth Syst. Sci.*, 22, 3765–3785, <https://doi.org/10.5194/nhess-22-3765-2022>, 2022b.
- 680 Ballantyne, C.K.: Paraglacial geomorphology, in: *Encyclopedia of Quaternary Science*, 3<sup>rd</sup> ed., Elsevier, 1–22, <https://doi.org/10.1016/b978-0-323-99931-1.00003-9>, 2022.
- Baurley, N.R., Robson, B.A., and Hart, J.K.: Long-term impact of the proglacial lake Jökulsárlón on the flow velocity and stability of Breiðamerkurjökull glacier, Iceland, *Earth Surf. Proc. Land.*, 45, 2647–2663, <https://doi.org/10.1002/esp.4920>, 2020.
- 685 Belart, J.M.C. and Magnússon, E.: Pléiades data as part of the CEOS Geohazard Supersites, <https://ceos.org/ourwork/workinggroups/disasters/gsnl/>, 2024.
- 690 Belart, J.M.C., Magnússon, E., Berthier, E., Gunnlaugsson, Á.Þ., Pálsson, F., Aðalgeirsdóttir, G., Jóhannesson, T., Thorsteinsson, T., and Björnsson, H.: Mass balance of 14 Icelandic glaciers, 1945–2017: Spatial variations and links with climate, *Front. Earth Sci.*, 8, 163, <https://doi.org/10.3389/feart.2020.00163>, 2020.
- Ben-Yehoshua, D., Sæmundsson, Þ., Helgason, J.K., Belart, J.M.C., Sigurðsson, J.V., and Erlingsson, S.: Paraglacial exposure and collapse of glacial sediment: The 2013 landslide onto Svínafellsjökull, southeast Iceland, *Earth Surf. Proc. Land.*, 47, 2612–2627, <https://doi.org/10.1002/esp.5398>, 2022.
- 695 Ben-Yehoshua, D., Sæmundsson, Þ., Helgason, J.K., Hermanns, R.L., Magnússon, E., Ófeigsson, B.G., Belart, J.M.C., Hjartardóttir, Á.R., Geirsson, H., Gu, S., and Hannesdóttir, H.: The destabilization of a large mountain slope controlled by thinning of Svínafellsjökull glacier, SE Iceland, *Jökull*, 73, 1–33, <https://doi.org/10.33799/jokull2023.73.001>, 2023.
- Benn, D.I., Warren, C.R., and Mottram, R.H.: Calving processes and the dynamics of calving glaciers. *Earth-Sci. Rev.*, 82, 143–179, <https://doi.org/10.1016/j.earscirev.2007.02.002>, 2007.
- 700 Bessette-Kirton, E.K. and Coe, J.A.: A 36-year record of rock avalanches in the Saint Elias Mountains of Alaska, with implications for future hazards, *Front. Earth Sci.*, 8, 293, <https://doi.org/10.3389/feart.2020.00293>, 2020.
- 705 Björnsson, H.: Subglacial lakes and jökulhlaups in Iceland, *Global Planet. Change*, 35, 255–271, [https://doi.org/10.1016/S0921-8181\(02\)00130-3](https://doi.org/10.1016/S0921-8181(02)00130-3), 2002.
- Björnsson, H., Pálsson, F., Gudmundsson, S., Magnússon, E., Aðalgeirsdóttir, G., Jóhannesson, T., Berthier, E., Sigurdsson, O., and Thorsteinsson, T.: Contribution of Icelandic ice caps to sea level rise: Trends and variability since the Little Ice Age, *Geophys. Res. Lett.*, 40, 1546–1550, <https://doi.org/10.1002/grl.50278>, 2013.
- 710 Böhme, M., Morken, O. A., Oppikofer, T., Hermanns, R. L., Penna, I., Nicolet, P., Bredal, M., Pullarello, J., and Noël, F.: Towards a national susceptibility map for rock avalanches, EGU General Assembly 2022, Vienna, Austria, 23–27 May 2022, EGU22-12124, <https://doi.org/10.5194/egusphere-egu22-12124>, 2022.
- 715 Bosson, J.B., Huss, M., Cauvy-Fraunié, S., Clément, J.C., Costes, G., Fischer, M., Poulenard, J., and Arthaud, F.: Future emergence of new ecosystems caused by glacial retreat, *Nature*, 620, 562–569, <https://doi.org/10.1038/s41586-023-06302-2>, 2023.

- Boyce, E.S., Motyka, R.J., and Truffer, M.: Flotation and retreat of a lake-calving terminus, Mendenhall Glacier, southeast Alaska, USA, *J. Glaciol.*, 53, 211–224, <https://doi.org/10.3189/172756507782202928>, 2007.
- 720 Bradwell, T.: Lichenometric dating in southeast Iceland: The size-frequency approach, *Geogr. Ann. A.*, 86, 31–41, <https://doi.org/10.1111/j.0435-3676.2004.00211.x>, 2004.
- Brown, C.S., Meier, M.F., and Post, A.: Calving speed of Alaska tidewater glaciers, with application to Columbia Glacier. *Geol. Surv. Prof. Pap.*, 1258-C, 1-13, 1982.
- 725 Byers, A.C., Rounce, D.R., Shugar, D.H., Lala, J.M., Byers, E.A., and Regmi, D.: A rockfall-induced glacial lake outburst flood, Upper Barun Valley, Nepal, *Landslides*, 16, 533–549, <https://doi.org/10.1007/s10346-018-1079-9>, 2019.
- 730 Carrivick, J.L. and Tweed, F.S.: Proglacial lakes: Character, behaviour and geological importance, *Quaternary Sci. Rev.*, 78, 34–52, <https://doi.org/10.1016/j.quascirev.2013.07.028>, 2013.
- Carrivick, J.L. and Tweed, F.S.: A global assessment of the societal impacts of glacier outburst floods, *Global Planet. Change*, 144, 1–16, <https://doi.org/10.1016/j.gloplacha.2016.07.001>, 2016.
- 735 Carrivick, J.L. and Tweed, F.S.: A review of glacier outburst floods in Iceland and Greenland with a megafloods perspective. *Earth-Sci. Rev.*, 196, 102876, <https://doi.org/10.1016/j.earscirev.2019.102876>, 2019.
- Carrivick, J.L. and Tweed, F.S.: Deglaciation controls on sediment yield: Towards capturing spatio-temporal variability, *Earth-Sci. Rev.*, 221, 103809, <https://doi.org/10.1016/j.earscirev.2021.103809>, 2021.
- 740 Carrivick, J.L., Tweed, F.S., Sutherland, J.L., and Mallalieu, J.: Toward numerical modeling of interactions between ice-marginal proglacial lakes and glaciers, *Front. Earth Sci.*, 8, 577068, <https://doi.org/10.3389/feart.2020.577068>, 2020.
- 745 Carrivick, J.L., Sutherland, J.L., Huss, M., Purdie, H., Stringer, C.D., Grimes, M., James, W.H.M., and Lorrey, A.M.: Coincident evolution of glaciers and ice-marginal proglacial lakes across the Southern Alps, New Zealand: Past, present and future, *Global Planet. Change*, 211, 103792, <https://doi.org/10.1016/j.gloplacha.2022.103792>, 2022.
- 750 Cathala, M., Magnin, F., Ravel, L., Dorren, L., Zuanon, N., Berger, F., Bourrier, F., and Deline, P.: Mapping release and propagation areas of permafrost-related rock slope failures in the French Alps: A new methodological approach at regional scale, *Geomorphology*, 448, 109032, <https://doi.org/10.1016/j.geomorph.2023.109032>, 2024.
- Chandler, B.M.P., Evans, D.J.A., Chandler, S.J.P., Ewertowski, M.W., Lovell, H., Roberts, D.H., Schaefer, M., and Tomczyk, A.M.: The glacial landsystem of Fjallsjökull, Iceland: Spatial and temporal evolution of process-form regimes at an active temperate glacier, *Geomorphology*, 361, 107192, <https://doi.org/10.1016/j.geomorph.2020.107192>, 2020.
- 755 Chigira, M.: September 2005 rain-induced catastrophic rockslides on slopes affected by deep-seated gravitational deformations, Kyushu, southern Japan, *Eng. Geol.*, 108, 1–15, <https://doi.org/10.1016/j.enggeo.2009.03.005>, 2009.
- Chigira, M., Tsou, C.-Y., Matsushi, Y., Hiraishi, N., and Matsuzawa, M.: Topographic precursors and geological structures of deep-seated catastrophic landslides caused by Typhoon Talas, *Geomorphology*, 201, 479–493, <https://doi.org/10.1016/j.geomorph.2013.07.020>, 2013.
- 760 Clague, J.J. and Evans, S.G.: A review of catastrophic drainage of moraine-dammed lakes in British Columbia, *Quaternary Sci. Rev.*, 19, 1763–1783, [https://doi.org/10.1016/s0277-3791\(00\)00090-1](https://doi.org/10.1016/s0277-3791(00)00090-1), 2000.
- Colonia, D., Torres, J., Haeberli, W., Schauwecker, S., Braendle, E., Giraldez, C., and Cochachin, A.: Compiling an inventory

- 765 of glacier-bed overdeepenings and potential new lakes in de-glaciating areas of the Peruvian Andes: Approach, first results, and perspectives for adaptation to climate change, *Water*, 9, 336, <https://doi.org/10.3390/w9050336>, 2017.
- Compagno, L., Zekollari, H., Huss, M., and Farinotti, D.: Limited impact of climate forcing products on future glacier evolution in Scandinavia and Iceland, *J. Glaciol.*, 67, 727–743, <https://doi.org/10.1017/jog.2021.24>, 2021.
- 770 Cook, S.J. and Quincey, D.J.: Estimating the volume of Alpine glacial lakes, *Earth Surf. Dynam.*, 3, 559–575, <https://doi.org/10.5194/esurf-3-559-2015>, 2015.
- Cook, S.J. and Swift, D.A.: Subglacial basins: Their origin and importance in glacial systems and landscapes, *Earth-Sci. Rev.*, 115, 332–372, <https://doi.org/10.1016/j.earscirev.2012.09.009>, 2012.
- 775 Cook, S.J., Kougkoulos, I., Edwards, L.A., Dortch, J., and Hoffmann, D.: Glacier change and glacial lake outburst flood risk in the Bolivian Andes, *Cryosphere*, 10, 2399–2413, <https://doi.org/10.5194/tc-10-2399-2016>, 2016.
- Czekirka, J., Westermann, S., Etzelmlüller, B., and Jóhannesson, T.: Transient modelling of permafrost distribution in Iceland, *Front. Earth Sci.*, 7, 130, <https://doi.org/10.3389/feart.2019.00130>, 2019.
- 780 Dai, C., Higman, B., Lynett, P.J., Jacquemart, M., Howat, I.M., Liljedahl, A.K., Dufresne, A., Freymueller, J.T., Geertsema, M., Ward Jones, M., and Haeussler, P.J.: Detection and assessment of a large and potentially tsunamigenic periglacial landslide in Barry Arm, Alaska, *Geophys. Res. Lett.*, 47, e2020GL089800, <https://doi.org/10.1029/2020GL089800>, 2020.
- 785 De Blasio, F.V.: Friction and dynamics of rock avalanches travelling on glaciers, *Geomorphology*, 213, 88–98, <https://doi.org/10.1016/j.geomorph.2014.01.001>, 2014.
- Delaney, K.B. and Evans, S.G.: The 1997 Mount Munday landslide (British Columbia) and the behaviour of rock avalanches on glacier surfaces, *Landslides*, 11, 1019–1036, <https://doi.org/10.1007/s10346-013-0456-7>, 2014.
- 790 Deline, P., Gruber, S., Amann, F., Bodin, X., Delaloye, R., Failletaz, J., Fischer, L., Geertsema, M., Giardino, M., Hasler, A., Kirkbride, M., Krautblatter, M., Magnin, F., McColl, S., Ravel, L., Schoeneich, P., Weber, S.: Ice loss from glaciers and permafrost and related slope instability in high-mountain regions, in: *Snow and Ice-Related Hazards, Risks, and Disasters*, 2<sup>nd</sup> ed., edited by: Haeberli, W. and Whiteman, C., Elsevier, 501–540, <https://doi.org/10.1016/B978-0-12-817129-5.00015-9>, 2021.
- 795 Deline, P., Hewitt, K., Shugar, D., and Reznichenko, N.: Rock avalanches onto glaciers, in: *Landslide Hazards, Risks, and Disasters*, 2<sup>nd</sup> ed., edited by: Davies, T., Rosser, N., and Shroder, J.F., Elsevier, 269–333, <https://doi.org/10.1016/B978-0-12-818464-6.00010-X>, 2022.
- 800 Dell, R., Carr, R., Phillips, E., and Russell, A.J.: Response of glacier flow and structure to proglacial lake development and climate at Fjallsjökull, south-east Iceland, *J. Glaciol.*, 65, 321–336, <https://doi.org/10.1017/jog.2019.18>, 2019.
- 805 Dunning, S.A., Large, A.R.G., Russell, A.J., Roberts, M.J., Duller, R., Woodward, J., Mériaux, A.-S., Tweed, F.S., and Lim, M.: The role of multiple glacier outburst floods in proglacial landscape evolution: The 2010 Eyjafjallajökull eruption, Iceland, *Geology*, 41, 1123–1126, <https://doi.org/10.1130/G34665.1>, 2013.
- Einarsson, P.: Historical accounts of pre-eruption seismicity of Katla, Hekla, Öräfajökull and other volcanoes in Iceland, *Jökull*, 69, 35–52, <https://doi.org/10.33799/jokull2019.69.035>, 2019.

- Emmer, A.: Vanishing evidence? On the longevity of geomorphic GLOF diagnostic features in the Tropical Andes, *Geomorphology*, 422, 108552, <https://doi.org/10.1016/j.geomorph.2022.108552>, 2023.
- 810 Emmer, A. and Vilímek, V.: Review article: Lake and breach hazard assessment for moraine-dammed lakes: An example from the Cordillera Blanca (Peru), *Nat. Hazards Earth Syst. Sci.*, 13, 1551–1565, <https://doi.org/10.5194/nhess-13-1551-2013>, 2013.
- 815 Emmer, A., Harrison, S., Mergili, M., Allen, S., Frey, H., and Huggel, C.: 70 years of lake evolution and glacial lake outburst floods in the Cordillera Blanca (Peru) and implications for the future, *Geomorphology*, 365, 107178, <https://doi.org/10.1016/j.geomorph.2020.107178>, 2020.
- 820 Emmer, A., Allen, S.K., Carey, M., Frey, H., Huggel, C., Korup, O., Mergili, M., Sattar, A., Veh, G., Chen, T.Y., Cook, S.J., Correas-Gonzalez, M., Das, S., Moreno, A.D., Drenkhan, F., Fischer, M., Immerzeel, W.W., Izagirre, E., Joshi, R.C., Kougkoulos, I., Knapp, R.K., Li, D., Majeed, U., Matti, S., Moulton, H., Nick, F., Piroton, V., Rashid, I., Reza, M., Ribeiro de Figueiredo, A., Riveros, C., Shrestha, F., Shrestha, M., Steiner, J., Walker-Crawford, N., Wood, J.L., and Yde, J.C.: Progress and challenges in glacial lake outburst flood research (2017-2021): A research community perspective, *Nat. Hazards Earth Syst. Sci.*, 22, 3041-3061, <https://doi.org/10.5194/nhess-22-3041-2022>, 2022.
- 825 Etzelmüller, B., Farbrót, H., Guðmundsson, Á., Humlum, O., Tveito, O.E., and Björnsson, H.: The regional distribution of mountain permafrost in Iceland, *Permafrost Periglac.*, 18, 185–199, <https://doi.org/10.1002/ppp.583>, 2007.
- 830 Etzelmüller, B., Patton, H., Schomacker, A., Czekirka, J., Girod, L., Hubbard, A., Lilleøren, K.S., and Westermann, S.: Icelandic permafrost dynamics since the Last Glacial Maximum – model results and geomorphological implications, *Quaternary Sci. Rev.*, 233, 106236, <https://doi.org/10.1016/j.quascirev.2020.106236>, 2020.
- Evans, S.G. and Clague, J.J.: Recent climatic change and catastrophic geomorphic processes in mountain environments, *Geomorphology*, 10, 107-128, [https://doi.org/10.1016/0169-555X\(94\)90011-6](https://doi.org/10.1016/0169-555X(94)90011-6), 1994.
- 835 Evans, D.J.A. and Twigg, D.R.: The active temperate glacial landsystem: A model based on Breiðamerkurjökull and Fjallsjökull, Iceland, *Quaternary Sci. Rev.*, 21, 2143–2177, [https://doi.org/10.1016/S0277-3791\(02\)00019-7](https://doi.org/10.1016/S0277-3791(02)00019-7), 2002.
- 840 Evans, S.G., Scarascia Mugnozza, G., Strom, A. L., Hermanns, R.L., Ischuk, A., and Vinnichenko, S.: Landslides from massive rock slope failure and associated phenomena, in: *Landslides from Massive Rock Slope Failure*, NATO Science Series, vol. 49, edited by: S.G. Evans, Scarascia Mugnozza, G., Strom, A.L., and Hermanns, R.L., Springer, 3-52, [https://doi.org/10.1007/978-1-4020-4037-5\\_1](https://doi.org/10.1007/978-1-4020-4037-5_1), 2006.
- Flowers, G.E., Marshall, S.J., Björnsson, H., and Clarke, G.K.C.: Sensitivity of Vatnajökull ice cap hydrology and dynamics to climate warming over the next 2 centuries, *J. Geophys. Res.-Earth*, 110, F02011, <https://doi.org/10.1029/2004JF000200>, 2005.
- 845 Frey, H., Haeberli, W., Linsbauer, A., Huggel, C., and Paul, F.: A multi-level strategy for anticipating future glacier lake formation and associated hazard potentials, *Nat. Hazards Earth Syst. Sci.*, 10, 339–352, <https://doi.org/10.5194/nhess-10-339-2010>, 2010.
- 850 Frey, H., Huggel, C., Chisolm, R.E., Baer, P., McArdeall, B., Cochachin, A., and Portocarrero, C.: Multi-source glacial lake outburst flood hazard assessment and mapping for Huaraz, Cordillera Blanca, Peru, *Front. Earth Sci.*, 6, 210, <https://doi.org/10.3389/feart.2018.00210>, 2018.
- Friðriksson, Á.: What is below the water masses? Multibeam studies of Öskjuvatn, Thingvallavatn and Kleifarvatn, Iceland, MS thesis, University of Iceland, 76 pp, 2014.

GAPHAZ, Assessment of Glacier and Permafrost Hazards in Mountain Regions – Technical Guidance Document, prepared by: Allen, S., Frey, H., Huggel, C., Bründl, M., Chiarle, M., Clague, J.J., Cochachin, A., Cook, S., Deline, P., Geertsema, M., Giardino, M., Haeberli, W., Kääb, A., Kargel, J., Klimes, J., Krautblatter, M., McArdell, B., Mergili, M., Petrakov, D., Portocarrero, C., Reynolds, J. and Schneider, D., Standing Group on Glacier and Permafrost Hazards in Mountains (GAPHAZ) of the International Association of Cryospheric Sciences (IACS) and the International Permafrost Association (IPA), Zurich, Switzerland / Lima, Peru, 72 pp, 2017.

Gantayat, P., Sattar, A., Haritashya, U.K., Ramsankaran, R., and Kargel, J.S.: Evolution of the Lower Barun lake and its exposure to potential mass movement slopes in the Nepal Himalaya, *Sci. Total Environ.*, 949, 175028, <https://doi.org/10.1016/j.scitotenv.2024.175028>, 2024a.

Gantayat, P., Sattar, A., Haritashya, U.K., Watson, C.S., and Kargel, J.S.: Bayesian approach to estimate proglacial lake volume (BE-GLAV), *Earth Sp. Sci.*, 11, e2024EA003542, <https://doi.org/10.1029/2024EA003542>, 2024b.

Geertsema, M., Menounos, B., Bullard, G., Carrivick, J.L., Clague, J.J., Dai, C., Donati, D., Ekstrom, G., Jackson, J.M., Lynett, P., Pichierri, M., Pon, A., Shugar, D.H., Stead, D., Del Bel Belluz, J., Friele, P., Giesbrecht, I., Heathfield, D., Millard, T., Nasonova, S., Schaeffer, A.J., Ward, B.C., Blaney, D., Blaney, E., Brillon, C., Bunn, C., Floyd, W., Higman, B., Hughes, K.E., McInnes, W., Mukherjee, K., and Sharp, M.A.: The 28 November 2020 landslide, tsunami, and outburst flood – a hazard cascade associated with rapid deglaciation at Elliot Creek, British Columbia, Canada, *Geophys. Res. Lett.*, 49, e2021GL096716, <https://doi.org/10.1029/2021GL096716>, 2022.

Golden Software, LLC: Surfer®, version 13, <https://www.goldensoftware.com>, 2015.

Grab, M., Mattea, E., Bauder, A., Huss, M., Rabenstein, L., Hodel, E., Linsbauer, A., Langhammer, L., Schmid, L., Church, G., Hellmann, S., Déléze, K., Schaer, P., Lathion, P., Farinotti, D., and Maurer, H.: Ice thickness distribution of all Swiss glaciers based on extended ground-penetrating radar data and glaciological modeling, *J. Glaciol.*, 67, 1074–1092, <https://doi.org/10.1017/jog.2021.55>, 2021.

Gruber, S. and Haeberli, W.: Permafrost in steep bedrock slopes and its temperature-related destabilization following climate change, *J. Geophys. Res.-Earth*, 112, F02S18, <https://doi.org/10.1029/2006JF000547>, 2007.

Guðmundsson, S., Björnsson, H., Pálsson, F., Magnússon, E., Sæmundsson, Þ., and Jóhannesson, T.: Terminus lakes on the south side of Vatnajökull ice cap, SE-Iceland, *Jökull*, 69, 1–34, <https://doi.org/10.33799/jokull2019.69.001>, 2019.

Gylfadóttir, S.S., Kim, J., Helgason, J.K., Brynjólfsson, S., Höskuldsson, Á., Jóhannesson, T., Harbitz, C.B., and Løvholt, F.: The 2014 Lake Askja rockslide-induced tsunami: Optimization of numerical tsunami model using observed data, *J. Geophys. Res.-Oceans*, 122, 4110–4122, <https://doi.org/10.1002/2016JC012496>, 2017.

Haeberli, W., Buetler, M., Huggel, C., Friedli, T.L., Schaub, Y., and Schleiss, A.J.: New lakes in deglaciating high-mountain regions – opportunities and risks, *Clim. Change*, 139, 201–214, <https://doi.org/10.1007/s10584-016-1771-5>, 2016.

Haeberli, W., Schaub, Y., and Huggel, C.: Increasing risks related to landslides from degrading permafrost into new lakes in de-glaciating mountain ranges, *Geomorphology*, 293, 405–417, <https://doi.org/10.1016/j.geomorph.2016.02.009>, 2017.

Hannesdóttir, H. and Guðmundsson, S.: Glacier outlines, Jöklavefsjá, <https://islenskirjoklar.is>, 2024.

Hannesdóttir, H., Björnsson, H., Pálsson, F., Aðalgeirsdóttir, G., and Guðmundsson, Sv.: Changes in the southeast Vatnajökull ice cap, Iceland, between ~1890 and 2010, *Cryosphere*, 9, 565–585, <https://doi.org/10.5194/tc-9-565-2015>, 2015.

- 905 Hannesdóttir, H., Sigurðsson, O., Prastarson, R.H., Guðmundsson, S., Belart, J.M.C., Pálsson, F., Magnússon, E., Víkingsson, S., Kaldal, I., and Jóhannesson, T.: A national glacier inventory and variations in glacier extent in Iceland from the Little Ice Age maximum to 2019, *Jökull*, 70, 1–34, <https://doi.org/10.33799/jokull.70.001>, 2020.
- Harbitz, C.B., Glimsdal, S., Løvholt, F., Kveldevik, V., Pedersen, G.K., and Jensen, A.: Rockslide tsunamis in complex fjords: From an unstable rock slope at Åkerneset to tsunami risk in western Norway, *Coast. Eng.*, 88, 101–122, <https://doi.org/10.1016/j.coastaleng.2014.02.003>, 2014.
- 910 Haritashya, U.K., Kargel, J.S., Shugar, D.H., Leonard, G.J., Strattman, K., Watson, C.S., Shean, D., Harrison, S., Mandli, K.T., and Regmi, D.: Evolution and controls of large glacial lakes in the Nepal Himalaya, *Remote Sens.*, 10, 798, <https://doi.org/10.3390/rs10050798>, 2018.
- 915 Harrison, S., Glasser, N., Winchester, V., Haresign, E., Warren, C., and Jansson, K.: A glacial lake outburst flood associated with recent mountain glacier retreat, *Patagonian Andes, Holocene*, 16, 611–620, <https://doi.org/10.1191/0959683606hl957rr>, 2006.
- 920 Harrison, S., Kargel, J.S., Huggel, C., Reynolds, J., Shugar, D.H., Betts, R.A., Emmer, A., Glasser, N., Haritashya, U.K., Klimeš, J., Reinhardt, L., Schaub, Y., Wiltshire, A., Regmi, D., and Vilímek, V.: Climate change and the global pattern of moraine-dammed glacial lake outburst floods, *Cryosphere*, 12, 1195–1209, <https://doi.org/10.5194/tc-12-1195-2018>, 2018.
- 925 Hartmeyer, I., Delleske, R., Keuschnig, M., Krautblatter, M., Lang, A., Schrott, L., and Otto, J.-C.: Current glacier recession causes significant rockfall increase: The immediate paraglacial response of deglaciating cirque walls, *Earth Surf. Dynam.*, 8, 729–751, <https://doi.org/10.5194/esurf-8-729-2020>, 2020.
- Hauksdóttir, H., Helgadóttir, E.G., and Guðmundsson, S.: Jarðfræðikortlagning á Breiðamerkursandi, Final report to the Student Innovation Fund, Náttúrustofa Suð austurlands, Höfn, Iceland, 26 pp., 2021. Helgason, J. and Duncan, R.A.: Glacial interglacial history of the Skaftafell region, Southeast Iceland, 0-5 Ma, *Geology*, 29, 179-182, [https://doi.org/10.1130/0091-7613\(2001\)029<0179:GIHOTS>2.0.CO;2](https://doi.org/10.1130/0091-7613(2001)029<0179:GIHOTS>2.0.CO;2), 2001.
- 930 Hermanns, R.L., Blikra, L.H., Naumann, M., Nilsen, B., Panthi, K.K., Stromeyer, D., and Longva, O.: Examples of multiple rock-slope collapses from Köfels (Ötztal valley, Austria) and western Norway, *Eng. Geol.*, 83, 94–108, <https://doi.org/10.1016/j.enggeo.2005.06.026>, 2006.
- 935 Hermanns, R.L., Blikra, L.H., Anda, E., Saintot, A., Dahle, H., Oppikofer, T., Fischer, L., Bunkholt, H., Böhme, M., Dehls, J.F., Lauknes, T.R., Redfield, T.F., Osmundsen, P.T., and Eiken, T.: Systematic mapping of large unstable rock slopes in Norway, in: *Landslide Science and Practice*, vol. 1, edited by: Margottini, C., Canuti, P., and Sassa, K., Springer, 29-34, [https://doi.org/10.1007/978-3-642-31325-7\\_3](https://doi.org/10.1007/978-3-642-31325-7_3), 2013.
- 940 Hermanns, R.L., Fauqué, L., and Wilson, C.G.J.:  $^{36}\text{Cl}$  terrestrial cosmogenic nuclide dating suggests Late Pleistocene to Early Holocene mass movements on the south face of Aconcagua mountain and in the Las Cuevas-Horcones valleys, *Central Andes, Argentina, Geol. Soc. Spec. Publ.*, 399, 345–368, <https://doi.org/10.1144/SP399.19>, 2015.
- Hermanns, R.L., Penna, I.M., Oppikofer, T., Noël, F., and Velardi, G.: Rock avalanche, in: *Treatise on Geomorphology*, vol. 5, 2<sup>nd</sup> ed., edited by: Shroder, J.F., Elsevier, 85–105, <https://doi.org/10.1016/B978-0-12-818234-5.00183-8>, 2022.
- 945 Higman, B., Shugar, D.H., Stark, C.P., Ekström, G., Koppes, N.M., Lynett, P., Dufresne, A., Haeussler, P.J., Geertsema, M., Gulick, S., Mattox, A., Venditti, J.G., Walton, M.A.L., McCall, N., Mckittrick, E., MacInnes, B., Bilderback, E.L., Tang, H., Willis, M.J., Richmond, B., Reece, R.S., Larsen, C., Olson, B., Capra, J., Ayca, A., Bloom, C., Williams, H., Bonno, D., Weiss, R., Keen, A., Skanavis, V., and Loso, M.: The 2015 landslide and tsunami in Taan Fiord, Alaska, *Sci. Rep.*,

8, 12993, <https://doi.org/10.1038/s41598-018-30475-w>, 2018.

950

Hilger, P., Hermanns, R.L., Gosse, J.C., Jacobs, B., Etzelmüller, B., and Krautblatter, M.: Multiple rock-slope failures from Mannen in Romsdal Valley, western Norway, revealed from Quaternary geological mapping and  $^{10}\text{Be}$  exposure dating, *Holocene*, 28, 1841–1854, <https://doi.org/10.1177/0959683618798165>, 2018.

955

Hock, R., Bliss, A., Marzeion, B.E.N., Giesen, R.H., Hirabayashi, Y., Huss, M., Radić, V., and Slangen, A.B.A.: GlacierMIP - A model intercomparison of global-scale glacier mass-balance models and projections, *J. Glaciol.*, 65, 453–467, <https://doi.org/10.1017/jog.2019.22>, 2019.

960

Hosmann, S.L., Fabbri, S.C., Buechi, M.W., Hilbe, M., Bauder, A., and Anselmetti, F.S.: Exploring beneath the retreating ice: swath bathymetry reveals sub- to proglacial processes and longevity of future alpine glacial lakes, *Ann. Glaciol.*, 1–6, <https://doi.org/10.1017/aog.2024.18>, 2024.

Howarth, P.J. and Price, R.J.: The Proglacial lakes of Breiðamerkurjökull and Fjallsjökull, Iceland, *Geogr. J.*, 135, 573–581, <https://doi.org/10.2307/1795105>, 1969.

965

Howat, I.M. and Eddy, A.L.: Multi-decadal retreat of Greenland’s marine-terminating glaciers, *J. Glaciol.*, 57, 389–396, <https://doi.org/10.3189/002214311796905631>, 2011.

970

Hubbard, B., Heald, A., Reynolds, J.M., Quincey, D., Richardson, S.D., Luyo, M.Z., Portilla, N.S., and Hambrey, M.J.: Impact of a rock avalanche on a moraine-dammed proglacial lake: Laguna Safuna Alta, Cordillera Blanca, Peru, *Earth Surf. Proc. Land.*, 30, 1251–1264, <https://doi.org/10.1002/esp.1198>, 2005.

975

Huggel, C., Kääb, A., Haeblerli, W., Teyssie, P., and Paul, F.: Remote sensing based assessment of hazards from glacier lake outbursts: A case study in the Swiss Alps, *Can. Geotech. J.*, 39, 316–330, <https://doi.org/10.1139/t01-099>, 2002.

Hugonnet, R., McNabb, R., Berthier, E., Menounos, B., Nuth, C., Girod, L., Farinotti, D., Huss, M., Dussailant, I., Brun, F., and Kääb, A.: Accelerated global glacier mass loss in the early twenty-first century, *Nature*, 592, 726–731, <https://doi.org/10.1038/s41586-021-03436-z>, 2021.

Hungr, O., Leroueil, S., and Picarelli, L.: The Varnes classification of landslide types, an update, *Landslides*, 11, 167–194, <https://doi.org/10.1007/s10346-013-0436-y>, 2014.

Icelandic Meteorological Office: Self service of weather observations, delivery no. 2024-06-04 13:08:24, 2024.

980

Jóhannesson, T., Björnsson, H., Magnússon, E., Guðmundsson, S., Pálsson, F., Sigurðsson, O., Thorsteinsson, T., and Berthier, E.: Ice-volume changes, bias estimation of mass-balance measurements and changes in subglacial lakes derived by lidar mapping of the surface of Icelandic glaciers, *Ann. Glaciol.*, 54, 63–74, <https://doi.org/10.3189/2013AoG63A422>, 2013.

985

Jóhannesson, T., Pálmason, B., Hjartarson, Á., Jarosch, A.H., Magnússon, E., Belart, J.M.C., and Guðmundsson, M.T.: Non-surface mass balance of glaciers in Iceland, *J. Glaciol.*, 66, 685–697, <https://doi.org/10.1017/jog.2020.37>, 2020.

990

Kapitsa, V., Shahgedanova, M., Kasatkin, N., Severskiy, I., Kasenov, M., Yegorov, A., and Tatko, M.: Bathymetries of proglacial lakes: A new data set from the northern Tien Shan, Kazakhstan, *Front. Earth Sci.*, 11, 1192719, <https://doi.org/10.3389/feart.2023.1192719>, 2023.

Keefer, D.K.: Landslides caused by earthquakes, *Bull. Geol. Soc. Am.*, 95, 406–421, 1984.



- Kershaw, J.A., Clague, J.J., and Evans, S.G.: Geomorphic and sedimentological signature of a two-phase outburst flood from moraine-dammed Queen Bess Lake, British Columbia, Canada, *Earth Surf. Proc. Land.*, 30, 1–25, <https://doi.org/10.1002/esp.1122>, 2005.
- 995 Kjartansson, G.: The Steinholtshlaup, central-south Iceland on January 15th, 1967, *Jökull*, 17, 249–262, 1967.
- Korup, O. and Dunning, S.: Catastrophic mass wasting in high mountains, in: *The High-Mountain Cryosphere: Environmental Changes and Human Risks*, edited by: Huggel, C., Carey, M., Clague, J.J., and Kääb, A., Cambridge University Press, 127–146, <https://doi.org/10.1017/CBO9781107588653.008>, 2015.
- 1000 Korup, O. and Tweed, F.: Ice, moraine, and landslide dams in mountainous terrain, *Quaternary Sci. Rev.*, 26, 3406–3422, <https://doi.org/10.1016/j.quascirev.2007.10.012>, 2007.
- Kos, A., Amann, F., Strozzi, T., Delaloye, R., von Ruette, J., and Springman, S.: Contemporary glacier retreat triggers a rapid landslide response, Great Aletsch Glacier, Switzerland, *Geophys. Res. Lett.*, 43, 12,466–12,474, <https://doi.org/10.1002/2016GL071708>, 2016.
- 1005 Krautblatter, M., Funk, D., and Günzel, F.K.: Why permafrost rocks become unstable: a rock–ice-mechanical model in time and space, *Earth Surf. Process. Landforms*, 38, 876–887, <https://doi.org/10.1002/esp.3374>, 2013.
- Krautblatter, M. and Leith, K.: Glacier- and permafrost-related slope instabilities, in: *The High-Mountain Cryosphere: Environmental Changes and Human Risks*, edited by: Huggel, C., Carey, M., Clague, J.J., and Kääb, A., Cambridge University Press, 147–165, <https://doi.org/10.1017/CBO9781107588653.009>, 2015.
- 1010 Lacroix, P., Belart, J.M.C., Berthier, E., Sæmundsson, Þ., and Jónsdóttir, K.: Mechanisms of landslide destabilization induced by glacier-retreat on Tungnakvíslarjökull area, Iceland, *Geophys. Res. Lett.*, 49, e2022GL098302, <https://doi.org/10.1029/2022GL098302>, 2022.
- 1015 Lala, J.M., Rounce, D.R., and McKinney, D.C.: Modeling the glacial lake outburst flood process chain in the Nepal Himalaya: Reassessing Imja Tsho’s hazard, *Hydrol. Earth Syst. Sci.*, 22, 3721–3737, <https://doi.org/10.5194/hess-22-3721-2018>, 2018.
- 1020 Landmælingar Íslands: ÍslandsDEM, <https://www.lmi.is>, 2021.
- Landmælingar Íslands: Aerial photo gallery, <https://www.lmi.is>, last access: 12 August 2022.
- Larsen, I.J. and Lamb, M.P.: Progressive incision of the Channeled Scablands by outburst floods, *Nature*, 538, 229–232, <https://doi.org/10.1038/nature19817>, 2016.
- 1025 Lea, J.M., Mair, D.W.F., and Rea, B.R.: Evaluation of existing and new methods of tracking glacier terminus change, *J. Glaciol.*, 60, 323–332, <https://doi.org/10.3189/2014JoG13J061>, 2014.
- Linsbauer, A., Frey, H., Haerberli, W., Machguth, H., Azam, M.F., and Allen, S.: Modelling glacier-bed overdeepenings and possible future lakes for the glaciers in the Himalaya-Karakoram region, *Ann. Glaciol.*, 57, 119–130, <https://doi.org/10.3189/2016AoG71A627>, 2016.
- 1030 Loftmyndir ehf.: <https://www.loftmyndir.is>, aerial photographs from 2003, 2025, 2019, and 2021, last access: 30 November 2022.

- 1035 Loriaux, T. and Casassa, G.: Evolution of glacial lakes from the Northern Patagonia Icefield and terrestrial water storage in a sea-level rise context, *Global Planet. Change*, 102, 33–40, <https://doi.org/10.1016/j.gloplacha.2012.12.012>, 2013.
- Lützow, N., Veh, G., and Korup, O.: A global database of historic glacier lake outburst floods, *Earth Syst. Sci. Data*, 15, 2983–3000, <https://doi.org/10.5194/essd-15-2983-2023>, 2023.
- 1040 Magnin, F., Haeberli, W., Linsbauer, A., Deline, P., and Raveland, L.: Estimating glacier-bed overdeepenings as possible sites of future lakes in the de-glaciating Mont Blanc massif (Western European Alps), *Geomorphology*, 350, 106913, <https://doi.org/10.1016/j.geomorph.2019.106913>, 2020.
- Magnússon, E., Björnsson, H., and Pálsson, F.: Landslag í grennd Kvískerja í fortíð og framtíð: Niðurstöður íssjármælinga á Kvíár-, Hrutár- og Fjallsjökli, *Jökull*, 57, 83–89, 2007.
- 1045 Magnússon, E., Pálsson, F., Björnsson, H., and Guðmundsson, S.: Removing the ice cap of Öraefajökull central volcano, SE-Iceland: Mapping and interpretation of bedrock topography, ice volumes, subglacial troughs and implications for hazards assessments, *Jökull*, 62, 131–150, 2012.
- 1050 Magnússon, E., Pálsson, F., Guðmundsson, M.T., Högnadóttir, T., Rossi, C., Thorsteinsson, T., Ófeigsson, B.G., Sturkell, E., and Jóhannesson, T.: Development of a subglacial lake monitored with radio-echo sounding: Case study from the eastern Skaftá cauldron in the Vatnajökull ice cap, Iceland, *Cryosphere*, 15, 3731–3749, <https://doi.org/10.5194/tc-15-3731-2021>, 2021.
- 1055 Main, B., Copland, L., Smeda, B., Kochtitzky, W., Samsonov, S., Dudley, J., Skidmore, M., Dow, C., Van Wychen, W., Medrzycka, D., Higgs, E., and Mingo, L.: Terminus change of Kaskawulsh Glacier, Yukon, under a warming climate: Retreat, thinning, slowdown and modified proglacial lake geometry, *J. Glaciol.*, 69, 936-952, <https://doi.org/10.1017/jog.2022.114>, 2022.
- 1060 Marzeion, B., Hock, R., Anderson, B., Bliss, A., Champollion, N., Fujita, K., Huss, M., Immerzeel, W.W., Kraaijenbrink, P., Malles, J.-H., Maussion, F., Radić, V., Rounce, D.R., Sakai, A., Shannon, S., van de Wal, R., and Zekollari, H.: Partitioning the uncertainty of ensemble projections of global glacier mass change, *Earth's Future*, 8, e2019EF001470, <https://doi.org/10.1029/2019EF001470>, 2020.
- 1065 Matthew, M.C., Gosse, J.C., Hermanns, R.L., Normandeau, A., and Tremblay, T.: Rock avalanches in northeastern Baffin Island, Canada: understanding low occurrence amid high hazard potential, *Landslides*, 21, 2307-2326, <https://doi.org/10.1007/s10346-024-02315-8>, 2024.
- Matti, S. and Ögmundardóttir, H.: Local knowledge of emerging hazards: Instability above an Icelandic glacier, *Int. J. Disaster Risk Reduct.*, 58, 102187, <https://doi.org/10.1016/j.ijdr.2021.102187>, 2021.
- 1070 Matti, S., Cullen, M., Reichardt, U., and Vigfúsdóttir, A.: Planned relocation due to landslide-triggered tsunami risk in recently deglaciated areas, *Int. J. Disaster Risk Reduct.*, 86, 103536, <https://doi.org/10.1016/j.ijdr.2023.103536>, 2023.
- 1075 McColl, S.T.: Paraglacial rock-slope stability, *Geomorphology*, 153–154, 1–16, <https://doi.org/10.1016/j.geomorph.2012.02.015>, 2012.
- Mergili, M., Pudasaini, S.P., Emmer, A., Fischer, J.-T., Cochachin, A., and Frey, H.: Reconstruction of the 1941 GLOF process chain at Lake Palcacocha (Cordillera Blanca, Peru), *Hydrol. Earth Syst. Sci.*, 24, 93–114, <https://doi.org/10.5194/hess-24-93-2020>, 2020.

- 1080 Minowa, M., Schaefer, M., and Skvarca, P.: Effects of topography on dynamics and mass loss of lake-terminating glaciers in southern Patagonia, *J. Glaciol.*, published online, 1–18. <https://doi.org/10.1017/jog.2023.42>, 2023.
- Mölg, N., Huggel, C., Herold, T., Storck, F., Allen, S., Haeberli, W., Schaub, Y., and Odermatt, D.: Inventory and evolution of glacial lakes since the Little Ice Age: Lessons from the case of Switzerland, *Earth Surf. Proc. Land.*, 46, 2551–2564, <https://doi.org/10.1002/esp.5193>, 2021.
- 1085 Moon, T. and Joughin, I.: Changes in ice front position on Greenland’s outlet glaciers from 1992 to 2007, *J. Geophys. Res.-Earth*, 113, F02022, <https://doi.org/10.1029/2007JF000927>, 2008.
- Moragues, S., Lenzano, M.G., Jeanneret, P., Gil, V., and Lannutti, E.: Landslide susceptibility mapping in the Northern part of Los Glaciares National Park, Southern Patagonia, Argentina using remote sensing, GIS and frequency ratio model, *Quaternary Science Advances*, 13., 100146, <https://doi.org/10.1016/j.qsa.2023.100146>, 2024.
- 1090 Morey, S.M., Shobe, C.M., Huntington, K.W., Lang, K.A., Johnson, A.G., and Duvall, A.R.: The lasting legacy of megaflood boulder deposition in mountain rivers, *Geophys. Res. Lett.*, 51, 1–11, <https://doi.org/10.1029/2023GL105066>, 2024.
- Motyka, R.J., Neel, S.O., Connor, C.L., and Echelmeyer, K.A.: Twentieth century thinning of Mendenhall Glacier, Alaska, and its relationship to climate, lake calving, and glacier run-off, *Global Planet. Change*, 35, 93–112, [https://doi.org/10.1016/S0921-8181\(02\)00138-8](https://doi.org/10.1016/S0921-8181(02)00138-8), 2002.
- 1095 Muñoz, R., Huggel, C., Frey, H., Cochachin, A., and Haeberli, W.: Glacial lake depth and volume estimation based on a large bathymetric dataset from the Cordillera Blanca, Peru. *Earth Surf. Proc. Land.*, 45, 1510–1527, <https://doi.org/10.1002/esp.4826>, 2020.
- 1100 Noël, B., Aðalgeirsdóttir, G., Pálsson, F., Wouters, B., Lhermitte, S., Haacker, J.M., and van den Broeke, M.R.: North Atlantic cooling is slowing down mass loss of Icelandic glaciers. *Geophys. Res. Lett.*, 49, e2021GL095697, <https://doi.org/10.1029/2021GL095697>, 2022.
- 1105 Oppikofer, T., Hermanns, R.L., Roberts, N.J., and Böhme, M.: SPLASH: Semi-empirical prediction of landslide-generated displacement wave run-up heights, *Geol. Soc. Spec. Publ.*, 477, <https://doi.org/10.1144/SP477.1>, 2018.
- Otto, J.-C., Helfricht, K., Prasicek, G., Binder, D., and Keuschnig, M.: Testing the performance of ice thickness models to estimate the formation of potential future glacial lakes in Austria, *Earth Surf. Proc. Land.*, 47, 723–741, <https://doi.org/10.1002/esp.5266>, 2022.
- 1110 Peng, M.: Measuring glacial lake bathymetry using uncrewed surface vehicles, *Nature Reviews Earth & Environment*, 4, 514, <https://doi.org/10.1038/s43017-023-00420-1>, 2023.
- Penna, I.M., Nicolet, P., Hermanns, R.L., Böhme, M., and Nöel, F.: Preliminary inventory of rock avalanche deposits and their related sources in Norway. Regional distribution, main features and topographic constraints, *Geological Survey of Norway*, Trondheim, Norway, 30 pp., 2022.
- 1115 Purdie, H., Gomez, C., and Espiner, S.: Glacier recession and the changing rockfall hazard: Implications for glacier tourism, *New Zeal. Geogr.*, 71, 189–202, <https://doi.org/10.1111/nzg.12091>, 2015.
- 1120 Purdie, H., Bealing, P., Tidey, E., Gomez, C., and Harrison, J.: Bathymetric evolution of Tasman Glacier terminal lake, New Zealand, as determined by remote surveying techniques, *Global Planet. Change*, 147, 1–11,

- 1125 Ramsankaran, R., Verma, P., Majeed, U., and Rashid, I.: Kayak-based low-cost hydrographic surveying system: A demonstration in high altitude proglacial lake associated with Drang Drung Glacier, Zaskar Himalaya, *J. Earth Syst. Sci.*, 132, 9, <https://doi.org/10.1007/s12040-022-02021-w>, 2023.
- 1130 Richardson, S.D. and Reynolds, J.M.: An overview of glacial hazards in the Himalayas. *Quatern. Int.*, 65–66, 31–47, [https://doi.org/10.1016/S1040-6182\(99\)00035-X](https://doi.org/10.1016/S1040-6182(99)00035-X), 2000.
- Rinzin, S., Zhang, G., Sattar, A., Wangchuk, S., Allen, S.K., Dunning, S., and Peng, M.: GLOF hazard, exposure, vulnerability, and risk assessment of potentially dangerous glacial lakes in the Bhutan Himalaya, *J. Hydrol.*, 619, 129311, <https://doi.org/10.1016/j.jhydrol.2023.129311>, 2023.
- 1135 Roberts, M.J. and Gudmundsson, M.T.: Öräfajökull volcano: Geology and historical floods, in: *Volcanogenic floods in Iceland: An assessment of hazards and risks at Öräfajökull and on the Markarfljót outwash plain*, edited by: Pagneux, E., Gudmundsson, M.T., Karlsdóttir, S., Roberts, and M.J., IMO, IES-UI, NCIP-DCPEM, Reykjavík, Iceland, 17–44, 2015.
- 1140 Roberts, M.J., Pálsson, F., Gudmundsson, M.T., Björnsson, H., and Tweed, F.S.: Ice-water interactions during floods from Grænalón glacier-dammed lake, Iceland, *Ann. Glaciol.*, 40, 133–138, <https://doi.org/10.3189/172756405781813771>, 2005.
- 1145 Roberts, N.J., McKillop, R.J., Lawrence, M.S., Psutka, J.F., Clague, J.J., Brideau, M.-A., and Ward, B.C.: Impacts of the 2007 landslide-generated tsunami in Chehalis Lake, Canada, in: *Landslide Science and Practice*, vol. 6., edited by: Margottini, C., Canuti, P., and Sassa, K., Springer, 133–140, [https://doi.org/10.1007/978-3-642-31319-6\\_19](https://doi.org/10.1007/978-3-642-31319-6_19), 2013.
- 1150 Romstad, B., Harbitz, C.B., and Domaas, U.: A GIS method for assessment of rock slide tsunami hazard in all Norwegian lakes and reservoirs, *Nat. Hazards Earth Syst. Sci.*, 9, 353–364, <https://doi.org/10.5194/nhess-9-353-2009>, 2009.
- Rounce, D.R., Hock, R., Maussion, F., Huggonet, R., Kochtitzky, W., Huss, M., Berthier, E., Brinkerhoff, D., Compagno, L., Copland, L., Farinotti, D., Menounos, B., and McNabb, R.W.: Global glacier change in the 21<sup>st</sup> century: Every increase in temperature matters, *Science*, 379, 78–83, <https://doi.org/10.1126/science.abo1324>, 2023.
- 1155 Russell, A.J., Roberts, M.J., Fay, H., Marren, P.M., Cassidy, N.J., Tweed, F.S., and Harris, T.: Icelandic jökulhlaup impacts: Implications for ice-sheet hydrology, sediment transfer and geomorphology, *Geomorphology*, 75, 33–64, <https://doi.org/10.1016/j.geomorph.2005.05.018>, 2006.
- 1160 Sattar, A., Goswami, A., Kulkarni, A.V., Emmer, A., Haritashya, U.K., Allen, S., Frey, H., and Huggel, C.: Future Glacial Lake Outburst Flood (GLOF) hazard of the South Lhonak Lake, Sikkim Himalaya, *Geomorphology*, 388, 107783, <https://doi.org/10.1016/j.geomorph.2021.107783>, 2021.
- Sattar, A., Allen, S., Mergili, M., Haeberli, W., Frey, H., Kulkarni, A.V., Haritashya, U.K., Huggel, C., Goswami, A., and Ramsankaran, R.: Modeling potential glacial lake outburst flood process chains and effects from artificial lake-level lowering at Gepang Gath Lake, Indian Himalaya, *J. Geophys. Res.-Earth*, 128, e2022JF006826, <https://doi.org/10.1029/2022JF006826>, 2023.
- 1165 Sæmundsson, P., Sigurðsson, I.A., Pétursson, H.G., Jónsson, H.P., Decaulne, A., Roberts, M.J., and Jensen, E.H.: Bergflóðið sem féll á Morsárjökul 20. mars 2007, *Náttúrufræðingurinn*, 81, 131–141, 2011.
- Schaub, Y., Huggel, C., Cochachin, A.: Ice-avalanche scenario elaboration and uncertainty propagation in numerical

simulation of rock-/ice-avalanche-induced impact waves at Mount Hualcán and Lake 513, Peru, *Landslides*, 13, 1445–1459, <https://doi.org/10.1007/s10346-015-0658-2>, 2016.

1170

Schmidt, L.S., Aðalgeirsdóttir, G., Pálsson, F., Langen, P.L., Guðmundsson, S., and Björnsson, H.: Dynamic simulations of Vatnajökull ice cap from 1980 to 2300, *J. Glaciol.*, 66, 97–112, <https://doi.org/10.1017/jog.2019.90>, 2020.

1175

Schomacker, A.: Expansion of ice-marginal lakes at the Vatnajökull ice cap, Iceland, from 1999 to 2009, *Geomorphology*, 119, 232–236, <https://doi.org/10.1016/j.geomorph.2010.03.022>, 2010.

1180

Shugar, D.H., Burr, A., Haritashya, U.K., Kargel, J.S., Watson, C.S., Kennedy, M.C., Bevington, A.R., Betts, R.A., Harrison, S., and Strattman, K.: Rapid worldwide growth of glacial lakes since 1990, *Nat. Clim. Change*, 10, 939–945, <https://doi.org/10.1038/s41558-020-0855-4>, 2020.

1185

Shugar, D.H., Jacquemart, M., Shean, D., Bhushan, S., Upadhyay, K., Sattar, A., Schwanghart, W., McBride, S., Van Wyk de Vries, M., Mergili, M., Emmer, A., Deschamps-Berger, C., McDonnell, M., Bhambri, R., Allen, S., Berthier, E., Carrivick, J.L., Clague, J.J., Dokukin, M., Dunning, S.A., Frey, H., Gascoin, S., Haritashya, U.K., Huggel, C., Kääb, A., Kargel, J.S., Kavanaugh, J.L., Lacroix, P., Petley, D., Rupper, S., Azam, M.F., Cook, S.J., Dimri, A.P., Eriksson, M., Farinotti, D., Fiddes, J., Gnyawali, K.R., Harrison, S., Jha, M., Koppes, M., Kumar, A., Leinss, S., Majeed, U., Mal, S., Muhuri, A., Noetzli, J., Paul, F., Rashid, I., Sain, K., Steiner, J., Ugalde, F., Watson, C.S., and Westoby, M.J.: A massive rock and ice avalanche caused the 2021 disaster at Chamoli, Indian Himalaya, *Science*, 373, 300–306, <https://doi.org/10.1126/science.abh4455>, 2021.

1190

Sigurðsson, O. and Williams, R.: Rockslides on the terminus of “Jökulsárgilsjökull”, southern Iceland, *Geogr. Ann. A*, 73, 129–140, <https://doi.org/10.2307/521018>, 1991.

1195

Somos-Valenzuela, M.A., McKinney, D.C., Byers, A.C., Rounce, D.R., Portocarrero, C., and Lamsal, D.: Assessing downstream flood impacts due to a potential GLOF from Imja Tsho in Nepal, *Hydrol. Earth Syst. Sci.*, 19, 1401–1412, <https://doi.org/10.5194/hess-19-1401-2015>, 2015.

1200

Sosio, R.: Rock–snow–ice avalanches, in: *Landslide Hazards, Risks, and Disasters*, edited by: Shroder, J.F. and Davies, T., Elsevier, 191–240, <https://doi.org/10.1016/B978-0-12-396452-6.00007-0>, 2015.

Sosio, R., Crosta, G.B., Chen, J.H., and Hungr, O.: Modelling rock avalanche propagation onto glaciers, *Quaternary Sci. Rev.*, 47, 23–40, <https://doi.org/10.1016/j.quascirev.2012.05.010>, 2012.

Steffen, T., Huss, M., Estermann, R., Hodel, E., and Farinotti, D.: Volume, evolution, and sedimentation of future glacier lakes in Switzerland over the 21st century, *Earth Surf. Dynam.*, 10, 723–741, <https://doi.org/10.5194/esurf-10-723-2022>, 2022.

1205

Stevenson, J.A., McGarvie, D.W., Smellie, J.L., and Gilbert, J.S.: Subglacial and ice-contact volcanism at the Öræfajökull stratovolcano, Iceland, *Bull. Volcanol.*, 68, 737–752, <https://doi.org/10.1007/s00445-005-0047-0>, 2006.

Stewart, E.J., Wilson, J., Espiner, S., Purdie, H., Lemieux, C., and Dawson, J.: Implications of climate change for glacier tourism, *Tourism Geog.*, 18, 377–398, <https://doi.org/10.1080/14616688.2016.1198416>, 2016.

1210

Stoffel, M. and Huggel, C.: Effects of climate change on mass movements in mountain environments, *Prog. Phys. Geog.*, 36, 421–439, <https://doi.org/10.1177/0309133312441010>, 2012.

1215

Storror, R.D., Jones, A.H., Evans, D.J.A.: Small-scale topographically-controlled glacier flow switching in an expanding proglacial lake at Breiðamerkurjökull, SE Iceland, *J. Glaciol.*, 63, 745–750, <https://doi.org/10.1017/jog.2017.22>, 2017.

- Strzelecki, M.C. and Jaskólski, M.W.: Arctic tsunamis threaten coastal landscapes and communities – survey of Karrat Isfjord 2017 tsunami effects in Nuugaatsiaq, western Greenland, *Nat. Hazards Earth Syst. Sci.*, 20, 2521–2534, <https://doi.org/10.5194/nhess-20-2521-2020>, 2020.
- 1220 Sutherland, J.L., Carrivick, J.L., Gandy, N., Shulmeister, J., Quincey, D.J., and Cornford, S.L.: Proglacial lakes control glacier geometry and behavior during recession, *Geophys. Res. Lett.*, 47, e2020GL088865, <https://doi.org/10.1029/2020GL088865>, 2020.
- Svennevig, K., Dahl-Jensen, T., Keiding, M., Boncori, J.P.M., Larsen, T.B., Salehi, S., Solgaard, A.M., and Voss, P.H.: Evolution of events before and after the 17 June 2017 rock avalanche at Karrat Fjord, West Greenland – a  
1225 multidisciplinary approach to detecting and locating unstable rock slopes in a remote Arctic area, *Earth Surf. Dynam.*, 8, 1021–1038, <https://doi.org/10.5194/esurf-8-1021-2020>, 2020.
- Svennevig, K., Hicks, S.P., Forbriger, T., Lecocq, T., Widmer-Schmidrig, R., Mangeney, A., Hibert, C., Korsgaard, N.J., Lucas, A., Satriano, C., Anthony, R.E., Mordret, A., Schippkus, S., Rysgaard, S., Boone, W., Gibbons, S.J., Cook, K.L., Glimsdal, S., Løvholt, F., Van Noten, K., Assink, J.D., Marboeuf, A., Lomax, A., Vanneste, K., Taira, T.,  
1230 Spagnolo, M., De Plaen, R., Koelemeijer, P., Ebeling, C., Cannata, A., Harcourt, W.D., Cornwell, D.G., Caudron, C., Poli, P., Bernard, P., Larose, E., Stutzmann, E., Voss, P.H., Lund, B., Cannavo, F., Castro-Díaz, M.J., Chaves, E., Dahl-Jensen, T., Pinho Dias, N. De, Déprez, A., Develter, R., Dreger, D., Evers, L.G., Fernández-Nieto, E.D., Ferreira, A.M.G., Funning, G., Gabriel, A.-A., Hendrickx, M., Kafka, A.L., Keiding, M., Kerby, J., Khan, S.A., Dideriksen, A.K., Lamb, O.D., Larsen, T.B., Lipovsky, B., Magdalena, I., Malet, J.-P., Myrup, M., Rivera, L., Ruiz-Castillo, E.,  
1235 Wetter, S., Wirtz, B.: A rockslide-generated tsunami in a Greenland fjord rang Earth for 9 days, *Science*, 385, 1196–1205, <https://doi.org/10.1126/science.adm9247>, 2024.
- Tang, M., Xu, Q., Wang, L., Zhao, H., Wu, G., Zhou, J., Li, G., Cai, W., and Chen, X.: Hidden dangers of ice avalanches and glacier lake outburst floods on the Tibetan Plateau: identification, inventory, and distribution, *Landslides*, 20,  
1240 2563–2581, <https://doi.org/10.1007/s10346-023-02125-4>, 2023.
- Thorarinsson, S.: The ice dammed lakes of Iceland with particular reference to their values as indicators of glacier oscillations, *Geogr. Ann.*, 21, 216–242, 1939.
- Thorarinsson, S.: Vatnajökull: scientific results of the Swedish–Icelandic investigations 1936–37–38. Chapter XI. Oscillations  
1245 of the Iceland glaciers in the last 250 years, *Geogr. Ann.*, 25, 1–54, 1943.
- Vieli, A.: Retreat instability of tidewater glaciers and marine ice sheets, in: *Snow and Ice-Related Hazards, Risks, and Disasters*, 2<sup>nd</sup> ed., edited by: Haeberli, W. and Whiteman, C., Elsevier, 671-706, <https://doi.org/10.1016/B978-0-12-817129-5.00009-3>, 2021.  
1250
- Welling, J. and Abegg, B.: Following the ice: Adaptation processes of glacier tour operators in Southeast Iceland, *Int. J. Biometeorol.*, 65, 703–715, <https://doi.org/10.1007/s00484-019-01779-x>, 2021.
- Welling, J., Árnason, Þ., and Ólafsdóttir, R.: Implications of climate change on nature-based tourism demand: A segmentation  
1255 analysis of glacier site visitors in southeast Iceland, *Sustainability*, 12, 5338, <https://doi.org/10.3390/su12135338>, 2020.
- Wells, G.H., Dugmore, A.J., Beach, T., Baynes, E.R.C., Sæmundsson, Þ., and Luzzadder-Beach, S.: Reconstructing glacial outburst floods (jökulhlaups) from geomorphology: Challenges, solutions, and an enhanced interpretive framework, *Prog. Phys. Geog.*, 46, 398–421, <https://doi.org/10.1177/03091333211065001>, 2022.  
1260
- Westoby, M.J., Glasser, N.F., Brasington, J., Hambrey, M.J., Quincey, D.J., and Reynolds, J.M.: Modelling outburst floods from moraine-dammed glacial lakes, *Earth-Sci. Rev.*, 134, 137–159, <https://doi.org/10.1016/j.earscirev.2014.03.009>,

2014a.

- 1265 Westoby, M.J., Glasser, N.F., Hambrey, M.J., Brasington, J., Reynolds, J.M., and Hassan, M.A.A.M.: Reconstructing historic  
Glacial Lake Outburst Floods through numerical modelling and geomorphological assessment: Extreme events in the  
Himalaya, *Earth Surf. Proc. Land.*, 39, 1675–1692, <https://doi.org/10.1002/esp.3617>, 2014b.
- 1270 Wieczorek, G.F., Geist, E.L., Motyka, R.J., and Jakob, M.: Hazard assessment of the Tidal Inlet landslide and potential  
subsequent tsunami, *Glacier Bay National Park, Alaska, Landslides*, 4, 205–215, <https://doi.org/10.1007/s10346-007-0084-1>, 2007.
- 1275 Wilson, R., Harrison, S., Reynolds, J., Hubbard, A., Glasser, N.F., Wünderlich, O., Iribarren Anaconda, P., Mao, L., and Shannon, S.: The 2015 Chileno Valley glacial lake outburst flood, Patagonia, *Geomorphology*, 332, 51–65, <https://doi.org/10.1016/j.geomorph.2019.01.015>, 2019.
- 1280 Worni, R., Huggel, C., and Stoffel, M.: Glacial lakes in the Indian Himalayas - From an area-wide glacial lake inventory to on-site and modeling based risk assessment of critical glacial lakes, *Sci. Total Environ.*, 468–469, S71–S84, <https://doi.org/10.1016/j.scitotenv.2012.11.043>, 2013.
- Worni, R., Huggel, C., Clague, J.J., Schaub, Y., and Stoffel, M.: Coupling glacial lake impact, dam breach, and flood processes: A modeling perspective, *Geomorphology*, 224, 161–176, <https://doi.org/10.1016/j.geomorph.2014.06.031>, 2014.
- 1285 Zemp, M., Huss, M., Thibert, E., Eckert, N., McNabb, R., Huber, J., Barandun, M., Machguth, H., Nussbaumer, S.U., Gärtner-Roer, I., Thomson, L., Paul, F., Maussion, F., Kutuzov, S., and Cogley, J.G.: Global glacier mass changes and their contributions to sea-level rise from 1961 to 2016, *Nature*, 568, 382–386, <https://doi.org/10.1038/s41586-019-1071-0>, 2019.
- 1290 Zhang, G., Carrivick, J.L., Emmer, A., Shugar, D.H., Veh, G., Wang, X., Labedz, C., Mergili, M., Mölg, N., Huss, M., Allen, S., Sugiyama, S., and Lützow, N.: Characteristics and changes of glacial lakes and outburst floods, *Nature Reviews Earth & Environment*, <https://doi.org/10.1038/s43017-024-00554-w>, 2024.
- 1295 Zheng, G., Allen, S.K., Bao, A., Ballesteros-Cánovas, J.A., Huss, M., Zhang, G., Li, J., Yuan, Y., Jiang, L., Yu, T., Chen, W., Stoffel, M.: Increasing risk of glacial lake outburst floods from future Third Pole deglaciation, *Nat. Clim. Change*, 11, 411–417, <https://doi.org/10.1038/s41558-021-01028-3>, 2021.
- Þórhallsdóttir, G.: Fjöldi í Vatnajökulspjóðgarði 2018 til 2022, *Vatnajökulspjóðgarður*, Höfn, Iceland, 299 pp., 2023.